Plant Stress 24 (2026) 101539

Contents lists available at ScienceDirect

Plant Stress

journal homepage: www.sciencedirect.com/journal/plant-stress

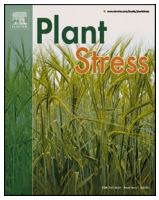

# Brassinosteroid seed priming enhances tolerance in a salt-sensitive sorghum through membrane, cell wall and $Na^+$ regulation

A. Peduzzi [a], D. Piacentini [a], S. D'Angeli [a], F. Sciubba [a,b], F. Marini [b,c], T. Napoleoni [a], E. Speranza [a], E. Eiche [d], M. Riemann [e], P. Nick [f], M.M. Altamura [a], G. Falasca [a,*]

[a] Department of Environmental Biology, Sapienza University of Rome, Italy
[b] NMR-Based Metabolomics Laboratory (NMLab), Sapienza University of Rome, Italy
[c] Department of Chemistry, Sapienza University of Rome, Italy
[d] Institute of Applied Geosciences, Karlsruhe Institute of Technology, Germany
[e] Department of Crop Sciences, FiBL Switzerland
[f] Molecular Cell Biology, Botanical Institute, Karlsruhe Institute of Technology, Germany

ARTICLE INFO

*Keywords:*
BR seed priming
Root development
NHX transporter
RAMAN micro-spectroscopy
Salt stress
*SbBRI-1*
*Sorghum bicolor*

ABSTRACT

Sorghum is generally considered a moderately salt-tolerant crop, although substantial variations in salt tolerance exist among grain sorghum genotypes. Moreover, the mechanisms underlying salt tolerance in this species remain poorly understood compared with those of other crops. Brassinosteroids (BRs) regulate numerous developmental processes and stress responses and their exogenous application, also via seed priming, has been shown to mitigate the negative effects of salinity in several plant species, including sorghum. However, the role of BR seed priming in root development and the biochemical, cellular, and molecular responses to salt stress remains unclear. Seeds of the salt-tolerant sorghum genotype Bianca and the salt-sensitive genotype Tonkawa were primed with 1μM of 24-epibrassinolide and then cultured *in vitro* in the presence or absence of 150 mM NaCl. Root system morphology, lipid peroxidation levels, Raman spectral profiles associated with membrane and cell wall components, cytosolic $K^+$ levels and vacuolar $Na^+$ compartmentalization were evaluated. BR seed priming enhanced root system architecture under salt stress, promoting adventitious and lateral root formation, and reducing lipid peroxidation, particularly in the salt-sensitive Tonkawa. In this genotype, BR seed priming had a long-lasting effect, inducing $Na^+$ sequestration in root cell vacuoles, modulating membrane and cell wall components, and improving root system branching, thereby ensuring adequate water uptake as a protective mechanism against high soil salinity. Overall, the results demonstrate the efficacy of BR seed priming in enhancing salt tolerance in sorghum, highlighting its potential as a sustainable strategy for improving crop performance under saline conditions.

## 1. Introduction

Rising temperatures driven by climate change represent one of the most critical environmental threats, accelerating soil degradation by increasing evapotranspiration, reducing soil moisture, and favoring desertification and soil salinization. Combined with unsustainable agricultural practices, these processes are jeopardizing food production in both arid and temperate regions worldwide. In 2021, it was estimated that 20% of total cultivated lands and 33% of irrigated agricultural lands were affected by high levels of salinity (Kraamwinkel et al., 2021). In Europe, a continent not typically associated with drought, soil salinization has been recognized as a factor contributing to soil degradation (Veerman et al., 2020). To cope with these challenges, agriculture needs to include underutilized crops with greater resilience, and sorghum seems to meet these needs.

*Sorghum bicolor* (L.) Moench has a large economic impact being among the five most widely cultivated crops globally. It is a multipurpose crop used for food, feed, fiber and fuel production. As a C4 plant, it can minimize resource losses due to photorespiration by closing the stomata during drought without compromising photosynthesis. In addition, its deep and extensive root system, thick leaf cuticles, and plasticity in root anatomy in response to stress, contribute to its ability to

* Corresponding author.
*E-mail address:* giuseppina.falasca@uniroma1.it (G. Falasca).

https://doi.org/10.1016/j.stress.2026.101539
Received 2 July 2026; Received in revised form 26 August 2026; Accepted 27 August 2026
Available online 27 August 2026

achieve osmotic adjustment while sustaining high photosynthetic efficiency under drought and salinity (Fracasso et al., 2017; Peduzzi et al., 2024; Peduzzi et al., 2025). These adaptations enable sorghum to maintain rapid growth even under conditions of low water availability (Kanbar et al., 2021). Thus, sorghum is considered one of the most promising cereal crops for cultivation in saline soils, where elevated salt concentrations decrease soil water potential, limiting water uptake by plants.

The threat posed by saline soils is primarily due to the presence of water-soluble salts, which dissociate in the soil solution, releasing free ions into the rhizosphere, where they can be readily taken up by plant roots. Among these, sodium ($Na^+$) and chloride ($Cl^-$) ions are particularly harmful to crops, as they can inhibit plant growth and, in severe cases, lead to plant death (Munns and Tester, 2008; Lindberg and Premkumar, 2024). Because plants have normally to maintain a tightly regulated balance of essential ions, including potassium ($K^+$), calcium ($Ca^{2+}$), and magnesium ($Mg^{2+}$), excessive accumulation of $Na^+$ and $Cl^-$ disrupts cellular ion homeostasis. When $Na^+$ exclusion and vacuolar compartmentalization are insufficient, $Na^+$ accumulates in the cytosol, competing with $K^+$ for transport and enzyme-binding sites (Ismail and Horie, 2017). These ionic imbalances impair cellular metabolism, disrupt photosynthetic and respiratory electron transport, and promote excessive production of reactive oxygen species (ROS), ultimately causing oxidative damage to cellular components (van Zelm et al., 2020). Thus, in response to high salt levels, plants activate several mechanisms to sequester and/or limit the diffusion of $Na^+$ ions. These mechanisms mainly involve transport systems that are crucial for maintaining cellular ion homeostasis, including high-affinity $K^+$ transporters (HKTs), $Na^+/H^+$ exchangers (NHXs), and the Salt Overly Sensitive (SOS) signaling pathway (van Zelm et al., 2020; Ma et al., 2026). The SOS pathway, composed of SOS3, SOS2, and SOS1, is a central regulatory module that senses cytosolic $Ca^{2+}$ signals induced by salt stress and activates the plasma membrane $Na^+/H^+$ antiporter SOS1, promoting $Na^+$ extrusion from root cells and thereby limiting its accumulation in the cytosol. HKTs mediate the transport of $Na^+$ and $K^+$ and are fundamental to maintain the balance between these ions. They contribute to $K^+$ uptake, which is essential for numerous physiological processes, including enzyme activation and osmoregulation (Nestrerenko et al., 2021). However, HKTs also exhibit a similar affinity for the toxic $Na^+$ ion. *HKT* genes are expressed in all plant organs and are often found in the xylem parenchyma (Riedelsberger et al. 2021). Indeed, in Arabidopsis, it has been suggested that AtHKT1;1 plays a role in the removal of $Na^+$ from the xylem sap thereby restricting its accumulation in the shoot (Sunarpi et al., 2005). Orthologues of this gene have been demonstrated to be essential for $Na^+$detoxification in important monocots, including wheat and rice (Hauser and Horie, 2010). The expression of *SbHKT1* was also observed to be higher in a salt-tolerant sorghum genotype than in a salt-sensitive one (Abuslima et al., 2022).

$Na^+/H^+$ vacuolar antiporters are other key transporters in maintaining ion homeostasis. These transporters, located on the tonoplast, sequester $Na^+$ ions into the vacuole, effectively reducing their cytoplasmic concentration and toxic effects on cellular structures (Jin et al., 2022; Waheed et al. 2024). In accordance, the over-expression of *AtNHX1* improves salt-tolerance in Arabidopsis and tomato, supporting the pivotal role of the vacuolar $Na^+/H^+$ antiporters in salt-tolerance (Shi and Zhu, 2002). Also, in wheat, higher expression of vacuolar $Na^+/H^+$ antiporters in roots and shoots has been associated with reduced root-to-shoot $Na^+$ translocation and greater tissue tolerance to $Na^+$ accumulation, thereby contributing to salt resistance (Saqib et al., 2005). In sorghum, sodium sequestration into the vacuole, due to *SbNHX2,* seems to play the main role in avoiding $Na^+$ translocation to the shoot (Abuslima et al., 2022).

At the whole-plant level, high soil salinity triggers a range of physiological alterations, including stomatal closure, hyper-osmotic shock, inhibition of cell division, nutrient imbalance, disruption of the reactive oxygen/nitrogen species (ROS/RNS) homeostasis, reduction of photosynthetic efficiency (Abdalla et al., 2022; Zhang et al., 2024; Peduzzi et al., 2025). Excessive ROS and RNS accumulation can damage cellular components, including membrane lipids, proteins, and DNA (Zhang et al., 2014; Ahmad et al., 2019). Thus, the activation of other adaptive mechanisms, such as root system plasticity, ROS scavenging and modulation in hormone levels or signalling, is essential for plant survival under saline conditions (Chawla et al., 2013; Karlova et al., 2021; Peduzzi et al. 2024).

Among phytohormones, brassinosteroids (BRs), a class of steroid hormones, play a central role in plant adaptation to salt stress by regulating ion homeostasis, antioxidant defence, cell wall remodelling, and root development. BR signalling is initiated by the perception of BRs by the plasma membrane receptor BRASSINOSTEROID INSENSITIVE 1 (BRI1) and its co-receptor BRI1-ASSOCIATED RECEPTOR KINASE 1 (BAK1), triggering a phosphorylation cascade that activates the transcription factors BRASSINAZOLE RESISTANT 1 (BZR1) and BRI1-EMS-SUPPRESSOR 1 (BES1). These transcriptional regulators control the expression of numerous genes involved in plant growth, development, and stress adaptation (Planas-Riverola et al., 2019; Kim and Russinova, 2020).

Under salt stress, BR signalling contributes to the maintenance of $Na^+/K^+$ homeostasis, $Na^+$ sequestration, ROS scavenging, root development, and cell wall remodelling, thereby enhancing plant salt tolerance (Anwar et al., 2018; Khan et al., 2023). Since BRI1 is the primary receptor for BR perception, alterations in its expression may affect the plant's capacity to perceive and transduce BR signals under salt stress. Consistent with this role, the Arabidopsis *bri1-9* mutant, which is defective in BR perception, exhibits increased sensitivity to salinity (Cui et al., 2012). Furthermore, in tomato plants exposed to high salinity, *SlBRI1* enhances salt tolerance by activating the antioxidant system and maintaining $Na^+/K^+$ homeostasis, and upregulating salt-responsive genes such as *NHX2* (Wang et al., 2023a). Although the physiological benefits of BR application under salinity are increasingly recognized, the molecular and cellular mechanisms through which BRs modulate root adaptive responses remain poorly understood, particularly in sorghum.

24-Epibrassinolide (24-eBL) is a biologically active BR involved in multiple plant processes, including stress responses to toxic metals and to other stressors (Ahanger et al., 2018; Della Rovere et al., 2025). 24-epibrassinolide can be applied exogenously through foliar spraying, seed priming, or via nutrient solutions, either *in planta* or in *in vitro* culture, to mitigate the effects of various abiotic stresses (Shahbaz and Ashraf 2007; Song et al. 2016; Piacentini et al., 2024; Allahverdian and Rahmani, 2025; Peduzzi et al. 2025). However, plant responses depend on the 24-eBL concentration, the application method, and the genotype. Hormone-mediated seed priming is defined as a pre-sowing treatment that enhances the plant responsiveness to subsequent stress without constitutive activation of defence responses (Conrath et al., 2015). Seed priming through the exogenous application of BRs (e.g., 24-eBL) represents a cost-effective, environmentally friendly, and scalable strategy for enhancing plant tolerance to abiotic stress. For example, in *Medicago sativa*, seed priming with 5 μM 24-eBL enhances seed germination in a saline soil and reduces the oxidative damage by improving the activity of superoxide dismutase, peroxidase and catalase (Zhang et al. 2007). In *Oryza sativa* Sharma et al. (2013) demonstrated that

$10^{-7}$ M 24-eBL was particularly effective in improving growth parameters, as well as protein, proline and antioxidant enzyme activities, while reducing malondialdehyde (MDA) content. Applications of 50 μg/L brassinolide to *in vitro* cultures of *Solanum tuberosum* plants improved $K^+/Na^+$ balance, root activity, and shoot antioxidative capacity under salt stress (Hu et al., 2016), and 24-eBL, applied as seed priming, restored the photosynthetic efficiency in a salt-sensitive sorghum genotype (Peduzzi et al. 2025). Despite the widely reported beneficial effects of exogenous 24-eBL seed priming, the specific cellular mechanisms underlying these effects in sorghum roots, particularly in

salt-sensitive genotypes, remain largely unexplored, as does their role in sustaining long-term salt tolerance.

The main aim of this study was to elucidate the mechanisms through which BRs, supplied via seed priming, enhance salt tolerance in sorghum by comparing the responses of the salt-tolerant genotype Bianca and the salt-sensitive genotype Tonkawa. Specifically, the study focused on early root traits, lipid peroxidation, Raman spectral signatures associated with membrane and cell wall components, $Na^+$ and $K^+$ homeostasis, and the expression of *SbBRI1, SbHKT*, and *SbNHX,* key genes involved in BR signalling and ion transport. The final goal was to provide a comprehensive understanding of the mechanisms underlying salt tolerance in sorghum and the potential benefits of 24-eBL seed priming, thereby supporting the development of environmentally sustainable strategies to enhance crop performance under saline conditions.

## 2. Materials and methods

### 2.1. Plant materials and growth conditions

Seeds of *Sorghum bicolor* (L.) Moench, genotypes Tonkawa and Bianca (provided by Padana Sementi Elette S.r.l.), were surface-sterilized and cultured *in vitro* in the absence (Control) or presence of 150 mM NaCl (NaCl) according to Peduzzi et al. (2024). Bianca and Tonkawa seeds were also primed with 1 μM of 24-epibrassinolide (24-eBL), a concentration selected based on the results reported by Peduzzi et al. (2025), and subsequently sown in either Control medium (P) or saline medium (P+NaCl). Both primed and non-primed seeds were sown under sterile conditions using a laminar flow hood and kept in a growth chamber under a long-day photoperiod (16 h light/8 h dark) for 6 or 10 days. The seeds were exposed to white light at an intensity of 150 μE $m^{-2}s^{-1}$ and maintained at controlled temperature (25°C light/24°C dark). Relative humidity inside the culture vessels was approximately 98–99 %. Twenty-seven seeds (9 per phytatray) were sown in three phytatrays for each treatment and genotype. After 24h from sowing the germination rate was also evaluated (Table S1). Three independent biological replicates were performed.

### 2.2. Morphological analyses

After 6 and 10 days from sowing, 15 seedlings per genotype and treatment (Control, NaCl, P, P+NaCl) were randomly selected, fixed in 70% ethanol and used for the evaluation of the mean primary root (PR) and adventitious roots (ARs) length and the mean number of ARs. The phenotype of the seedlings after 10 days of culture under the different treatment conditions is shown in Fig. S1. The root systems were scanned using a high-resolution scanner (Expression 1200 x l, Epson, Japan), the images were acquired with Epson Scan software (Epson, Japan) and processed with ImageJ v1.53c software (Wayne Rasband, National Institutes of Health, Bethesda, USA). Primary roots and ARs were measured using RootNav v1.8.1 software (Pound et al., 2013). One AR from each of fifteen 10-day-old seedlings was selected for the evaluation of lateral root primordia (LRPs) density, expressed as the total number of LRPs per cm of AR. To assess the effects of BR seed priming on shoot development, fresh shoot biomass and the mean number of leaves were evaluated in 15 seedlings per genotype and treatment 10 days after sowing. These analyses were repeated for each of the three biological replicates.

### 2.3. Lipid peroxidation analysis

Lipid peroxidation was evaluated by quantifying the level of malondialdehyde (MDA), a major by-product generated during lipid peroxidation. Malondialdehyde levels were determined by quantifying thiobarbituric acid-reactive substances (TBARS). The TBARs assay was performed according to Heath and Packer (1968). Three seedlings from each genotype and treatment were harvested at day 10 after sowing, divided into shoots and roots, and homogenized with liquid nitrogen. Aliquots of 100 mg per sample were collected and extracted in 1mL of 0.1% trichloroacetic acid (TCA). The extraction solution was centrifuged for 10 min at 10,000 x g at room temperature. The supernatant was collected and added to 4mL of the reaction solution (0.5% thiobarbituric acid, and 20% TCA). The reaction was activated by incubating the samples in a stirring bath (WB-4MS, Biosan, Latvia) at 95°C for 30 min and then stopped by placing the tubes on ice for 10 min. The solution was centrifuged at 10,000 x g for 5 min, and the supernatant was used to measure the absorbance at 532 and 600 nm, within the following 30 min, using Colibri+ spectrophotometer (Berthold Technologies GmbH & Co. KG, Germany). MDA content was determined by subtracting the absorbance at 600 nm from that at 532 nm and using a calibration curve created with different MDA (Sigma-Aldrich, Germany) standard concentrations (1μM, 2μM, 5μM, 10μM, 20μM, 50μM). Results were expressed as nmol MDA $g^{-1}$ FW and represent the mean ±SE values from three technical replicates.

### 2.4. RNA extraction and quantitative real-time PCR

The root system was separated from the shoot in 6-day-old and 10-day-old seedlings, and the total RNA was extracted from both shoots and roots using 100 mg of fresh tissue. RNA was extracted using the InnuPrep Plant RNA kit (Analytika Jena RNA kit) according to the manufacturer's instructions. RNA was then purified with DNase (NEB, UK) digestion, and its purity was assessed using a NanoDrop spectrophotometer and by gel electrophoresis to verify the absence of DNA bands. Reverse transcription into cDNA was performed on 1 μg of RNA per sample, using the cDNA synthesis protocol M-Mulv-Reverse transcriptase (NEB, UK) according to Peethambaran et al., (2018). Real-time PCR was performed using a SYBR green dye protocol on a CFX Connect Real-Time PCR System (Bio-Rad, USA), using Ubiquitin (*SbUBQ*) as internal reference gene. Each 20 μL reaction mixture contained 11.75 μL of nuclease-free water, 4 μL of GoTaq buffer, 0.4 μL of dNTPs (10 mM), each of forward and reverse primers (1:10 diluted), 1 μL of $MgCl_2$ (50 mM), 0.95 μL of SYBR Green, 0.1 μL of GoTaq Polymerase, and 1μL of cDNA (1:49 diluted). The primer sequences used to amplify the genes of interest (*SbNHX2, SbHKT1*, and *SbBRI1*) are reported in Table S2. The transcript levels of samples were calculated using the $2^{-\Delta Ct}$ method to obtain expression levels normalized to the reference gene without the use of a calibrator sample (Schmittgen and Livak, 2008). Data represent the mean gene expression values (±SE) from three independent biological replicates; each measured in triplicates.

### 2.5. Raman micro-spectroscopy analysis

Raman spectra were acquired using an InVia Renishaw spectrometer (2400 lines/mm grarting) (Renishaw, UK) equipped with a 532 nm laser beam with a maximum power of 50 mW used as the excitation source. The laser beam was redirected on a Zeiss LSM900 confocal scanning laser microscope (Zeiss, Germany), provided with a 63x immersion objective for image and spectra acquisition.

For each analysis the spectral region of 500 to 1800 $cm^{-1}$ was considered, and the spectra were acquired as the sum of 100 accumulations with an exposure time of 1 s per accumulation.

The Raman spectra were corrected using the Savitzky-Golay smoothing algorithm and the baseline correction by means of the Wire 5.6 software (Renishaw).

To identify the most representative peaks, Raman spectra were acquired from root homogenates treated with aqueous solutions containing increasing concentrations of 24-eBL (0, $10^{-6}$ M and $10^{-4}$ M) and pure water. The intensities of four peaks (882 $cm^{-1}$, 1050 $cm^{-1}$, 1450 $cm^{-1}$and 1730 $cm^{-1}$ Raman Shift) were correlated with 24-eBL concentrations in the roots of both genotypes. These peaks were used as reference Raman bands to assess treatment-related trends.

Three ARs, per genotype and treatment, were used for Raman analysis. Three different root regions, adventitious root meristem (ARM), lateral root meristem (LRM) and AR differentiated zone (epidermis, E, and cortical parenchyma cells, C) (Fig. S2) were used as source for spectral acquisition. The mean peak area was calculated for each measurement point and Raman shift.

### 2.6. Determination of $Na^+$ and $K^+$ content

The $Na^+$ and $K^+$ contents were determined in the roots and shoots of seedlings grown for 6 and 10 days under Control conditions, NaCl treatment, 24-eBL priming (P), and 24-eBL priming followed by NaCl treatment (P+NaCl). Oven-dried roots and shoots (at 48°C for 2 days, ~50 mg) were placed in 50 mL digestion tubes (Gerhardt, UK) containing 1 mL ultrapure water, 2 mL $HNO_3$ (65% v/v, subboiled) and 0.25 mL $H_2O_2$ (30% v/v, p.A.). Subsequently, the tubes were closed and incubated in a heating block (DigiPrepjr, S-prep) system at 110°C for 2h. After cooling, the digests were quantitatively transferred to volumetric flasks and brought to a final volume of 10 mL with 1% (v/v) $HNO_3$. To verify the quality of the digestion and quantification procedure, both in the digestion and in the quantification processes, blank samples and two reference materials (tomato leaves - NIST 1573a; grass - 14th needle/leaf inter laboratory test) (Abuslima et al. 2022) were included. The accuracy was mainly in a range of ± 5-10%. Sodium and potassium ions were quantified by Inductively Coupled Plasma Optical Emission Spectrometry (ICP-OES; iCap7000, Thermo Fisher; Varian), using both axial and radial mode. The precision (<±3%) and accuracy (mainly <±3.5%) of the ICP-OES measurements was assessed using the MISA 6 CRM /VHG. Data were expressed as mg $g^{-1}$ DW and represent the mean (±SE) of three biological replicates.

### 2.7. Detection of vacuolar and cytosolic $Na^+$ distribution across different root zones

The cellular compartmentalization of $Na^+$ ions was examined in cells of the mature and meristematic root zones using CoroNa™ Green AM fluorescent dye (Invitrogen, Thermo Fisher Scientific, USA) according to Wu et al., 2015. Three ARs of comparable length (~2.5cm) and developmental stage were collected from three different 10-day-old seedlings of each genotype grown under Control, NaCl or P+NaCl treatments. The roots were rinsed with ultrapure water and used for $Na^+$ localization. To simultaneously visualise $Na^+$ ions and the plasma and vacuolar membranes, the roots were double-stained with 20 µM CoroNa™ Green-AM and 20 µM FM™4-64 membrane-selective dye (Invitrogen, Thermo Fisher Scientific, USA), for 2 hours in the dark at 37°C. The samples were then rinsed with 5 mM MES buffer (pH 6.3) to remove unbound probes. Confocal analysis was performed using a Zeiss Imager M2 microscope equipped with a Zeiss LSM 900 confocal laser scanning unit (Zeiss, Germany). Images were acquired in multichannel mode using either a 20x (Plan Apochromat 0.8 M27) or a 40x objective lens (W Plan Apochromat Korr 0.95 M27) operated through the ZEN 3.1 software (Zeiss, Germany), using identical acquisition settings (laser power, pinhole, pixel, exposure time, and gain) to ensure comparability between samples. Laser excitation wavelengths of 488 nm for CoroNa Green-AM and 561 nm for FM4-64 were used, with fluorescence emission collected using 450–533 nm and 656–700 nm bandpass filters, respectively, as exemplified in Fig. S3. Mean fluorescence signal intensity in the cytoplasm and vacuoles of differentiated and meristematic root cells was determined using ImageJ software (https://imagej.nih.gov/ij/) and expressed as arbitrary units (AUs) (Abuslima et al., 2022). Data represent the mean fluorescence signal (±SE) from 45 cells per root zone, treatment, and genotype, obtained from the three independent biological replicates.

### 2.8. Statistical analyses

All the data obtained from the above-mentioned measurements were tested for normality using the Shapiro-Wilk's test and subsequently analysed by two-way ANOVA test followed by Šídák's multiple comparison test. Comparison was performed among treatments within the same genotype and time point, with statistical significance set at $p < 0.05$ (Stevens, 2007). The statistical analyses were carried out through GraphPad Prism 9.3.0 software (GraphPad Software, San Diego, CA, USA).

#### 2.8.1. ANOVA-simultaneous component analysis (ASCA) for Raman analysis

Multivariate analysis of the Raman data acquired in the 500–1800 $cm^{-1}$ region was performed using ANOVA-Simultaneous Component Analysis (ASCA) (Smilde et al., 2005), a chemometric method that combines the partitioning capabilities of analysis of variance (ANOVA) with the dimensionality reduction properties of principal component analysis (PCA). The software used was MATLAB R2026 (MathWorks, USA).

Given the hierarchical structure of the experimental design, ASCA was performed through a series of separate models. First, the two genotypes (Bianca and Tonkawa) were analysed independently, considering treatment (Control, NaCl, P, and P+NaCl) and root region and tissues (ARM, LRM, epidermis, and cortex) as fixed factors in a two-way ASCA design. Subsequently, separate ASCA models were built for each root region, considering genotype and treatment as factors, to evaluate genotype-dependent responses within specific compartments. Prior to analysis, the Raman data matrix was normalized by standard normal variate (SNV) transformation (Barnes et al., 1989) and mean-centered. The ASCA decomposition generated effect matrices associated with each factor and their interaction, which were subsequently explored by Principal Component Analysis (PCA). The statistical significance of the effects was assessed by permutation testing (10,000 permutations) (Vis et al., 2007). Score plots were used to visualize treatment- and genotype-related patterns, while loading profiles were examined to identify the Raman bands most strongly contributing to the observed differences.

Since statistical significance of the ASCA effects was evaluated through permutation testing rather than by relying on the parametric F distribution of classical ANOVA, no preliminary tests of univariate normality or homogeneity of variance were performed. The permutation scheme was defined consistently with the experimental design to preserve exchangeability under the null hypothesis.

## 3. Results

### 3.1. 24-eBL seed priming improves post-embryonic root system development in the salt- sensitive Tonkawa under salt stress

To evaluate the effects of 24-eBL seed priming (P) on root system development, the mean primary root (PR) length, as well as the number and length of adventitious roots (ARs), were measured in both genotypes at 6 and 10 days after sowing. In Bianca, the PR length was unaffected by either NaCl or seed priming treatments at either time point (Fig. 1a-b). By contrast, in Tonkawa, the salt treatment significantly reduced PR length compared with the Control as early as 6 days after sowing, and this inhibitory effect persisted through day 10. Moreover, 24-eBL seed priming was unable to restore PR elongation impaired by salt toxicity (Fig. 1a-b).

At day 6, the NaCl treatment induced a marked reduction in AR formation in both genotypes in comparison with the Control, with a more pronounced effect in Tonkawa (Fig. 1c). In Bianca, the P treatment did not significantly affect AR number in comparison with the Control. On the contrary, when followed by NaCl treatment (P+NaCl), it induced a significant ($p<0.0001$) increase in the AR mean number in comparison

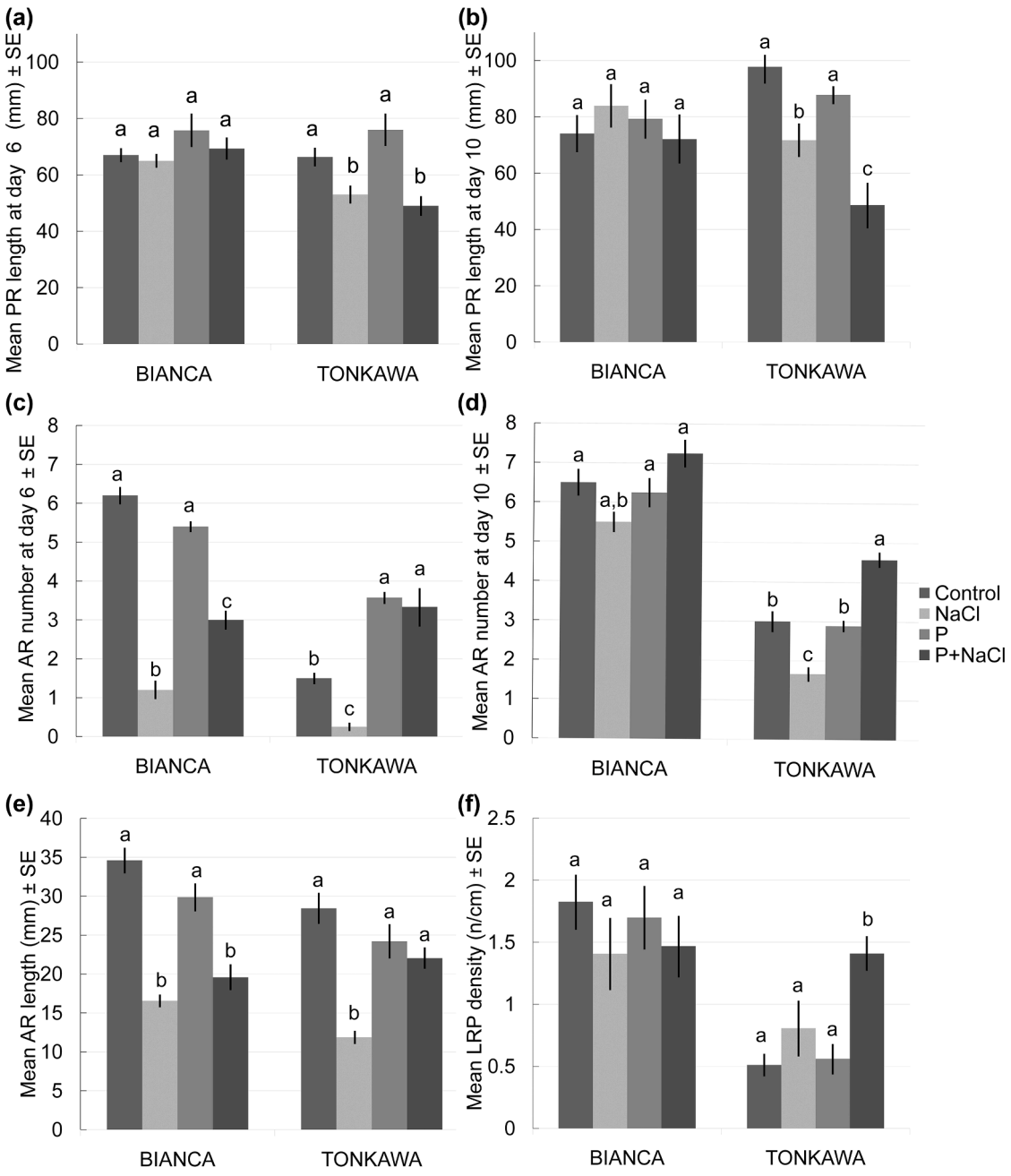


**Fig. 1.** Root system morphology at 6 (a, c) and 10 (b, d-f) days from sowing in Bianca and Tonkawa non-primed and not exposed to NaCl (Control), non-primed and exposed to 150 mM NaCl (NaCl), primed only (P) and primed and exposed to NaCl (P + NaCl). (a-b), mean primary root (PR) length (±SE); (c-d), mean adventitious root (AR) number (±SE); (e), mean adventitious root (AR) length (±SE); (f), mean lateral root primordia (LRPs) density (±SE). Different letters show significant differences among treatments within the same genotype for at least $p < 0.05$. The same letter shows no significant difference within the same genotype. N=15.

with NaCl alone, although the values remained below those of the Control (Fig. 1c).

Tonkawa generally produced fewer ARs than Bianca. However, 6 days after sowing, the number of ARs was significantly ($p < 0.0001$) higher under P and P+ NaCl treatments than under NaCl and Control conditions (Fig. 1c).

At day 10 after sowing, salt treatment did not significantly reduce AR formation in Bianca, confirming the greater tolerance of this genotype to salt stress. Neither P nor P+NaCl treatments significantly changed the AR mean number in comparison with the Control (Fig. 1d). Conversely, in Tonkawa, NaCl significantly ($p < 0.05$) reduced AR formation at day 10 after sowing (Fig. 1d). The priming followed by NaCl induced a significant ($p < 0.0001$) increase in AR formation compared with both NaCl and Control treatments (Fig. 1d). Thus, in Tonkawa, AR formation showed a strong and early recovery in the seedlings primed with 24-eBL compared with those exposed to NaCl.

To further characterize the effects of salinity and of 24-eBL seed priming on the sorghum root system, the mean AR length and lateral root primordia (LRPs) density were measured in the 10-day-old seedlings.

The mean AR length was significantly ($p<0.001$) reduced by NaCl treatment in both genotypes (Fig. 1e). The seed priming with 24-eBL followed by the NaCl treatment significantly restored NaCl-impaired AR growth in Tonkawa, but not in Bianca seedlings (Fig. 1e). In Bianca, no significant differences in LRP density were observed regardless of the treatments (Fig. 1f), whereas in Tonkawa, the P+NaCl

treatment strongly increased LRP formation, in comparison with both Control and NaCl treatments (Fig. 1f).

To evaluate the effect of 24-eBL seed priming on shoot development, the shoot biomass and the mean leaf number were measured in 10-day-old seedlings.

Shoot development was strongly affected by salt in both genotypes, as evidenced by reduced shoot biomass and leaf number (Fig. 2a-b). However, a positive effect of the seed priming on the leaf number was observed in Tonkawa but not in Bianca (Fig. 2b).

Overall, 24-eBL seed priming effectively mitigates salt-induced damage to the root system during post-embryonic development, particularly in the salt-sensitive genotype Tonkawa, by enhancing AR growth and increasing LRP density. Seed priming also improved shoot development by increasing leaf number in salt-stressed Tonkawa seedlings.

### 3.2. 24-eBL seed priming reduces salt stress-induced lipid peroxidation in roots and shoots

It is known that salt stress induces reactive oxygen species (ROS) accumulation in sorghum roots, particularly in the salt-sensitive genotype Tonkawa (Peduzzi et al., 2024). Since ROS can cause extensive oxidative damage, including lipid peroxidation of cellular membranes, we investigated whether 24-eBL seed priming was able to mitigate these detrimental effects. Thus, a spectrophotometric TBARS assay was performed to quantify the lipid peroxidation marker MDA in the roots and shoots of 10-day-old seedlings. Results showed that the MDA levels increased in both roots (Fig. 3a) and shoots (Fig. 3b) of Bianca and Tonkawa after NaCl treatment. However, these increases were significant ($p < 0.001$) compared with the Control only in Tonkawa. When the P treatment was followed by NaCl, a marked reduction in the MDA content was observed in both roots and shoots of the two genotypes, reaching levels comparable to those of the Control (Fig. 3a-b). However, in Tonkawa shoots, the decrease in MDA was less pronounced than in Bianca (Fig. 3b).

Overall, these results highlight that salt increased lipid peroxidation in both roots and shoots, with higher levels observed in Tonkawa than in Bianca. Moreover, the 24-eBL seed priming was effective in reducing lipid peroxidation, particularly in Tonkawa roots.

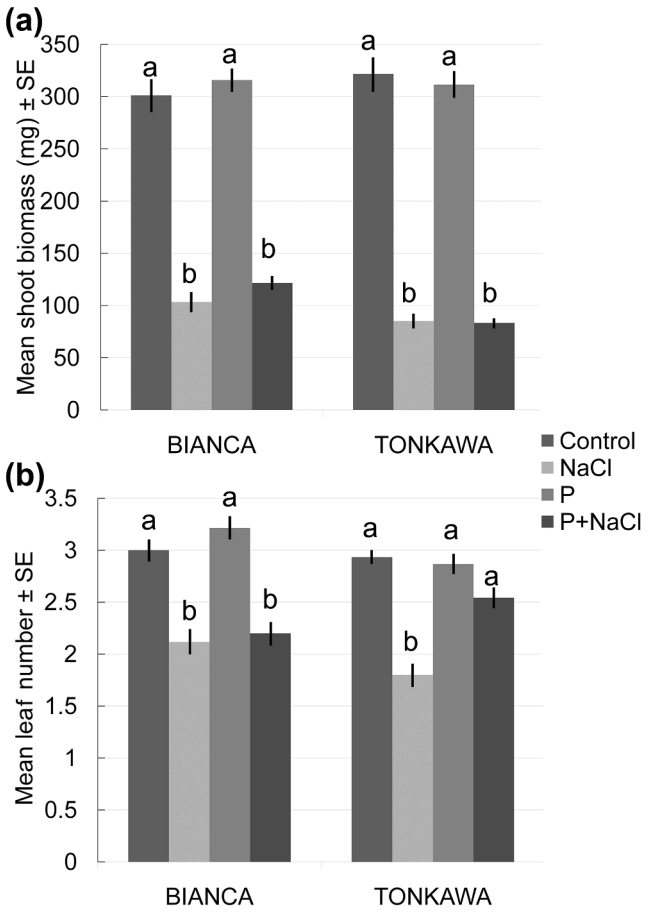


**Fig. 2.** Mean shoot biomass (±SE) (a) and mean number of leaves (±SE) (b) after 10 days from sowing in Bianca and Tonkawa seedlings non-primed and not exposed to NaCl (Control), non-primed and exposed to 150 mM NaCl (NaCl), primed only (P) and primed and exposed to NaCl (P + NaCl). Different letters show significant differences among treatments within the same genotype for at least $p < 0.05$. The same letter shows no significant difference within the same genotype. N=15.

### 3.3. 24-eBL seed priming induces long-lasting changes in endogenous SbBRI1 transcript abundance

To determine whether 24-eBL seed priming induced long-lasting changes in BR perception-related gene expression and contributed to sorghum responses to salt stress, we evaluated the expression of *SbBRI1* gene, which encodes the main BR receptor, in roots and shoots of both genotypes at 6 and 10 days from sowing.

Six days after sowing, the two genotypes showed similar trends in *SbBRI1* expression, in the two organs, in response to the different treatments (Fig. 4a-b). *SbBRI1* expression was higher in the shoots than in the roots of Control and NaCl-treated seedlings. Salt stress reduced *SbBRI1* expression in the roots while increasing it in the shoot, mainly in Bianca. In contrast, P treatment did not significantly affect *SbBRI1* expression with transcript levels remaining comparable to those observed in the Control (Fig. 4a-b). When 24-eBL seed priming was followed by NaCl treatment, *SbBRI1* expression levels were comparable to those of the Control in both organs and in both genotypes (Fig. 4 a-b).

Ten days after sowing, *SbBRI1* transcript abundance was higher in roots and lower in shoots than at day 6 in both genotypes and under all treatments, except for NaCl alone (Fig. 4c-d). In Tonkawa roots,10 days after sowing, the expression of this gene was significantly reduced by NaCl treatment ($p < 0.01$) compared with all other treatments (Fig. 4d). Seed priming, both alone and followed by NaCl treatment, significantly ($p<0.05$) increased gene expression in comparison with the NaCl-alone treatment, restoring expression levels to those observed under Control conditions (Fig. 4d).

These results show that *SbBRI1* expression was higher in shoots than in roots at 6 days after sowing, whereas this pattern reversed at 10 days in both genotypes. In fact, at day 10, salt treatment reduced *SbBRI1* expression in roots but not in shoots in both genotypes, with a significant effect observed only in Tonkawa. Notably, 24-eBL seed priming restored *SbBRI1* expression to levels comparable to those of the Control.

### 3.4. 24-eBL seed priming induces genotype-dependent long-term changes in root cell wall and membrane components

Using Raman micro-spectroscopy, we checked for the presence of chemical changes induced by 24-eBL seed priming in the root cells of Bianca and Tonkawa. The analysis was carried out on single cells belonging to the AR meristem (ARM), LRP meristematic cells (LRM) and differentiated epidermal (E) and cortical (C) root cells (Fig. S2).

Raman spectra acquired from the different root cell types showed numerous vibrational peaks (data not shown). To identify the most representative peaks, Raman spectra were also acquired from root-cell homogenates supplemented with aqueous solutions containing increasing concentrations of 24-eBL (0, $10^{-6}$ and $10^{-4}$M). The obtained spectra revealed four peaks whose intensities varied with the applied 24-eBL concentrations or with water. Specifically, the peak at 882 $cm^{-1}$, consistent with β-glycosidic (C–O–C) and polysaccharide skeletal vibrations (mainly cellulose/hemicellulose) (Gierlinger et al., 2012; Clark

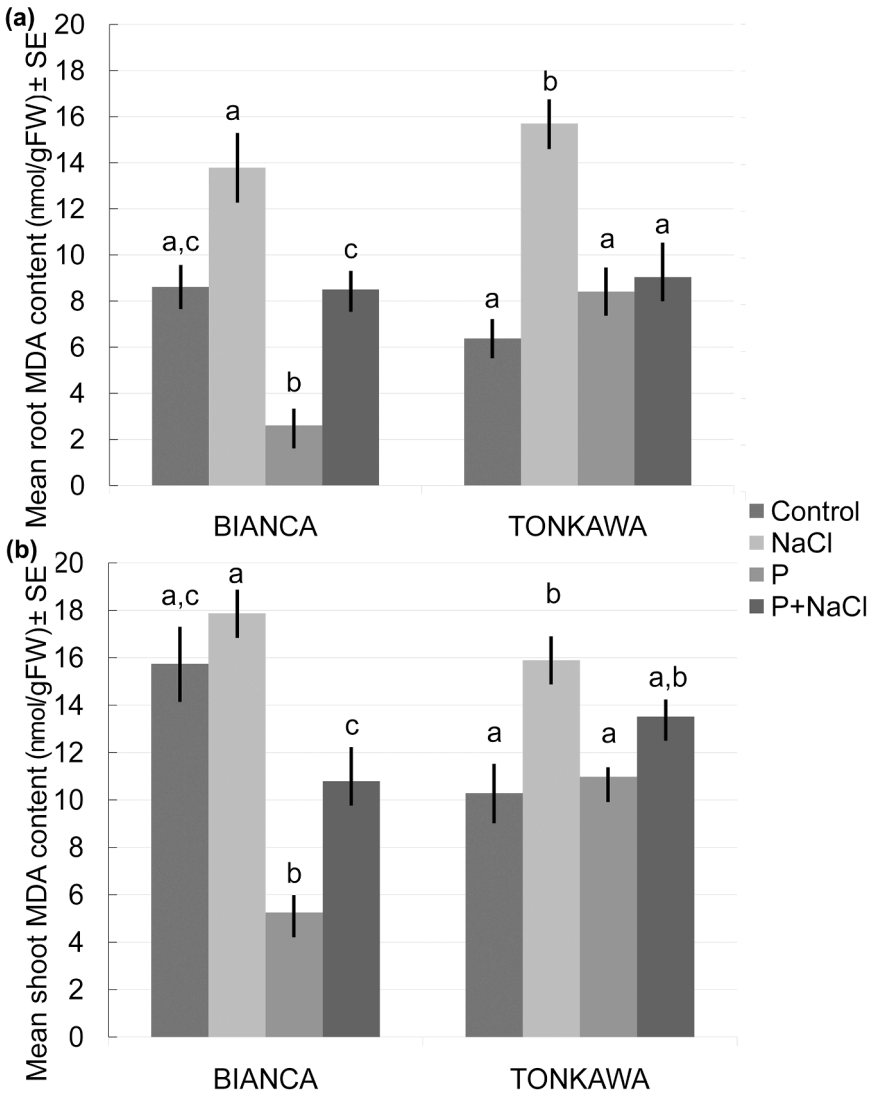


**Fig. 3.** Malondialdehyde (MDA) content in the root system (a) and in the shoot (b) of Bianca and Tonkawa 10-day-old seedlings non-primed and not exposed to NaCl (Control), non-primed and exposed to 150 mM NaCl (NaCl), primed only (P) and primed and exposed to NaCl (P + NaCl). Different letters represent statistically significant differences among treatments within the same genotype for at least $p<0.05$. The same letter shows no significant difference within the same genotype. N=9.

and Goldberg Oppenheimer, 2024); 1050 $cm^{-1}$, attributed to C–O and C–C stretching vibrations of polysaccharides (mainly cellulose) (Zeise et al., 2018; Gieroba et al., 2023); 1450 $cm^{-1}$, assigned to $CH_2/CH_3$ bending vibrations of lipids, proteins, and other aliphatic components (Clark and Goldberg Oppenheimer, 2024); and 1730 $cm^{-1}$, attributed to C=O stretching vibrations of ester groups (Payne and Kurouski, 2021), were identified (Fig. 5a). The values of the integrated areas of these peaks were calculated and expressed in arbitrary units (AUs).

The integrated areas of the selected Raman peaks varied among the sorghum root samples of both genotypes exposed to the different treatments (Fig. 5b-c). In the Control meristematic cells (ARM and LRMs) of the ARs and LRPs, respectively, of both genotypes, higher values were observed for the peaks commonly associated with lipids and proteins (1450 $cm^{-1}$), whereas in the differentiated cells (epidermis and cortex) higher values were observed for peaks corresponding to carbohydrates and ester groups (1050 and 1730 $cm^{-1}$). By contrast, the integrated area of the 882 $cm^{-1}$ peak, consistent with stretching vibrations associated with cellulose and hemicellulose, was low and similar across cell types, genotypes and treatments (Fig. 5b-c). The salt alone treatment induced an increase in the 1050 $cm^{-1}$peak area in the epidermis and cortical parenchyma cells, compared to the Control treatment in both genotypes but with a more pronounced effect in Tonkawa than in Bianca. Higher integrated area values of the 1450 $cm^{-1}$ peak were observed in Bianca roots than in Tonkawa roots. However, in meristematic cells (ARM and LRM) of Tonkawa roots, exposed to P+NaCl treatment, the area values of this peak were higher than in the corresponding cells of Bianca (Fig. 5b-c). Moreover, only in Tonkawa the peak area values at 1450 and 1730 $cm^{-1}$ in meristematic cells decreased following salt exposure in comparison with those measured in the meristematic root cells of the Control (Fig. 5b-c). Priming alone induced an increase in the peak area associated with ester groups in differentiated epidermis and cortical parenchyma cells, as well as in the peak at 1450 $cm^{-1}$ in the ARM cells of Bianca. By contrast, in Tonkawa, priming alone led to a decrease in peak area values across all the analyzed cell types (Fig. 5b-c). Priming followed by salt treatment showed reduced peak areas across all cell types in Bianca, with values lower than those observed under the salt treatment alone and, in some cases, comparable to those of the Control (Fig. 5b). In Tonkawa, instead, peak area values at 1450 $cm^{-1}$ increased relatively to those observed under the salt treatment alone, reaching levels comparable to the Control in ARMs and exceeding Control in LRMs (Fig. 5c). Similarly, the peak area values at 1730 $cm^{-1}$ reached values like to those of the Control in ARMs and

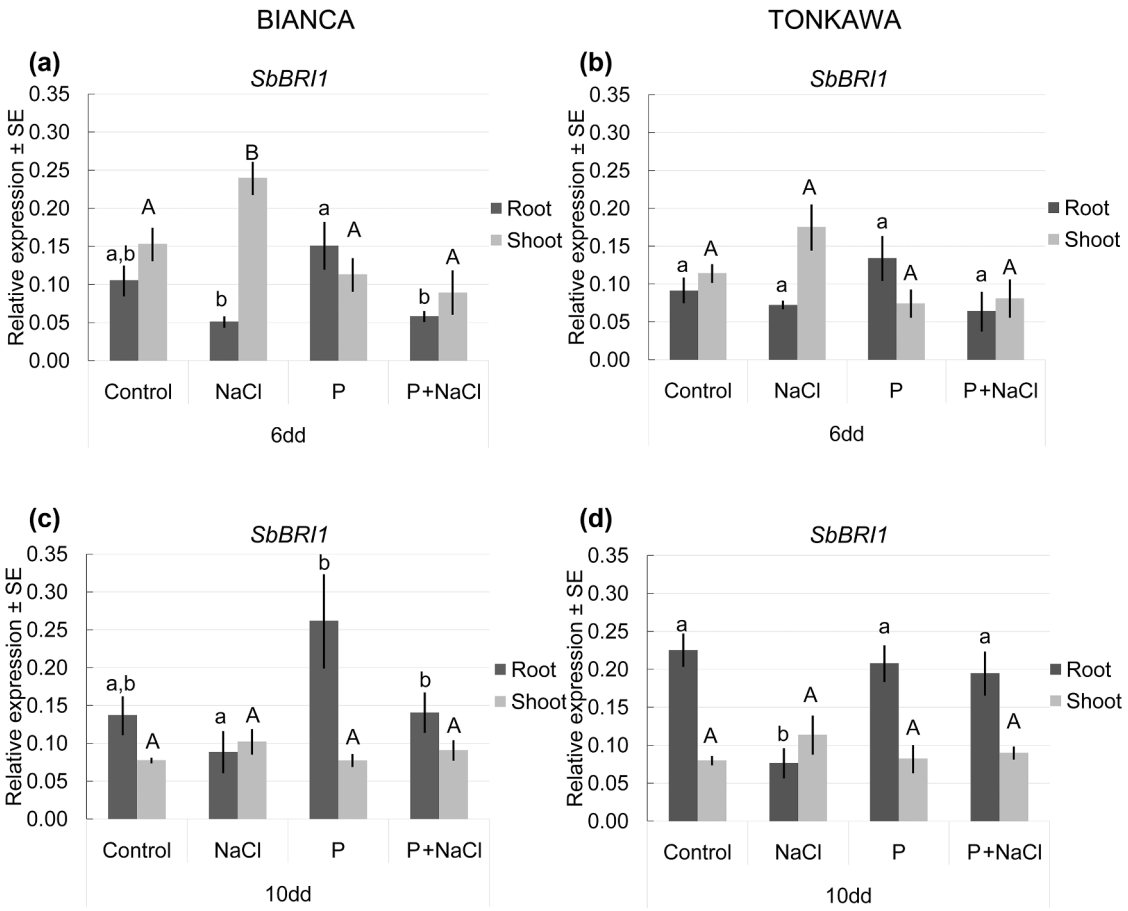


**Fig. 4.** Relative expression of *SbBRI1*, encoding the main brassinosteroid (BR) receptor, after 6 (a–b) and 10 (c–d) days after sowing, in the shoots and roots of Bianca and Tonkawa seedlings non-primed and not exposed to NaCl (Control), non-primed and exposed to 150 mM NaCl (NaCl), primed only (P) and primed and exposed to NaCl (P + NaCl). Transcript abundance was normalized to *SbUBQ*. Different lowercase letters indicate significant differences among treatments in roots, while different uppercase letters indicate significant differences among treatments in shoots for at least $p<0.05$. The same letter shows no significant difference within the same genotype and organ. **N=9.**

higher than Control levels in LRMs (Fig. 5c).

To complement the analysis of these selected Raman bands and obtain a more comprehensive overview of the biochemical responses induced by 24-eBL priming and salt stress, the full Raman spectra were also analyzed using ASCA. This approach allowed the spectral variability to be partitioned according to the experimental factors and their interactions, thereby revealing multivariate patterns that could not be captured by the analysis of individual Raman bands.

When the two genotypes were analyzed separately, with treatment and root tissue considered as factors, all effects (i.e., treatment, root tissue and their interaction) were statistically significant ($p < 0.0001$). In both Bianca and Tonkawa, root tissue represented the major source of spectral variation, accounting for 33.96% and 26.97% of the total variance, respectively (Fig. S4). Treatment effects explained a smaller but still significant portion of the variance, particularly in Tonkawa (8.56% and 10.49% respectively) (Fig. S4). The treatment × root tissue interaction explained 12.73% and 15.29% of the variance in Bianca and Tonkawa, respectively (Fig. S4). These results indicate that the biochemical composition of the different root tissues is the dominant determinant of the Raman fingerprint, whereas treatment-induced changes depend strongly on the specific tissue analyzed.

To further investigate genotype-dependent responses, separate ASCA models were developed for each root tissue using genotype and treatment as factors. In the ARM region, treatment significantly affected the Raman profiles (10.06% explained variance; $p = 0.0148$), whereas the genotype effect was not significant, indicating that both genotypes responded similarly in this compartment (Fig. 6a). Conversely, in the LRM, epidermis and cortex, both genotype and treatment effects were highly significant ($p < 0.0001$), together with their interaction (Fig. 6b-d). The strongest genotype effect was observed in the LRM, where genotype accounted for 23.25% of the total variance, highlighting substantial biochemical differences between Bianca and Tonkawa in this meristematic region (Fig. 6b).

Inspection of the corresponding loading profiles (data not shown) indicated that the observed discrimination was mainly driven by Raman bands associated with polysaccharide vibrations and membrane-associated lipid and ester components, consistent with the patterns identified by univariate analysis of the 882, 1050, 1450, and 1730 $cm^{-1}$ bands.

Overall, Raman analysis and ASCA elaborations sustain that 24-eBL priming induces long-lasting biochemical modifications in sorghum roots and that these modifications are strongly influenced by both genotype and root tissue. In particular, the salt stress enhances the intensity of Raman bands associated with cell wall carbohydrates in differentiated cells, especially in Tonkawa. Conversely, 24-eBL seed priming improved Tonkawa root cells response to salt stress, restoring the Raman signals associated with cell wall carbohydrates, cell membrane proteins, and lipids to Control levels across all analysed cell types.

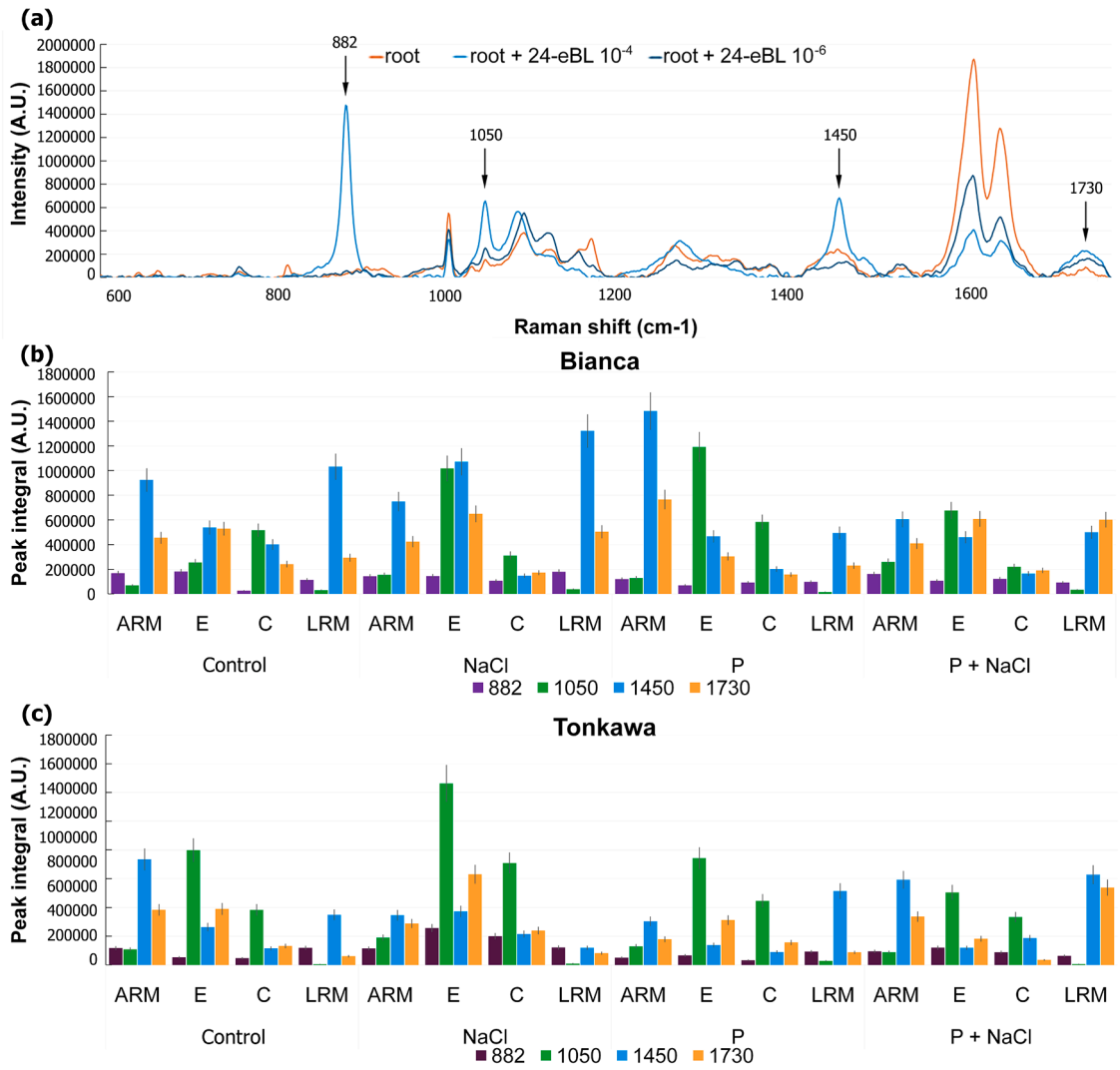


**Fig. 5.** (a) Raman spectra acquired from the root-cell homogenate supplemented with aqueous solutions containing 0 M (root), $10^{-6}$ M (root + 24-eBL $10^{-6}$M) and $10^{-4}$M (root + 24-eBL $10^{-4}$M) of 24-eBL. (b-c) Mean integrated areas of the selected peaks from spectra acquired from 10-day-old roots of Bianca (b) and Tonkawa (c) seedlings non-primed and not exposed to NaCl (Control), non-primed and exposed to 150 mM NaCl (NaCl), primed only (P) and primed and exposed to NaCl (P + NaCl). Spectra were acquired from four different tissues: AR meristem (ARM), LRP meristematic cells (LRM) and differentiated epidermal (E) and cortical (C) root cells. Integrated band areas are expressed in arbitrary units (AUs). Error bars indicate ±10% percentage error.

### *3.5. 24-eBL seed priming modulates the expression of $Na^+$ and $Na^+/K^+$ transporter genes*

To verify whether the effects of 24-eBL seed priming were associated with changes in the expression of genes involved in $Na^+$ compartmentalization and $Na^+/K^+$ homeostasis, the expression of the *SbNHX2* and *SbHKT1* genes, encoding a vacuolar $Na^+/H^+$ antiporter and a membrane high-affinity $K^+$ transporter, respectively, was evaluated in roots and shoots after 6 and 10 days from sowing.

After 6 days of salt exposure, *SbNHX2* expression was lower in the roots than in the shoots of both Bianca and Tonkawa, except in P-treated seedlings (Fig. S5a-b). Moreover, *SbHKT1* expression was detected at very low levels in the roots and was almost undetectable in the shoots of both genotypes. No significant differences among treatments were detected for either gene in the roots or shoots of either genotype at this time point (Fig. S5c-d).

Ten days after sowing, *SbNHX2* expression in both roots and shoots of Bianca was unaffected by the treatments and showed no evident change compared with day 6 (Figs. 7a and S5a in comparison). In contrast, in Tonkawa, the gene expression increased in roots and decreased in shoots, compared with day 6 (Figs. 7b and S5b in comparison). However, NaCl treatment significantly reduced *SbNHX2* expression in roots in comparison with the Control (Fig. 7b). It should be underlined that, in Tonkawa roots, P+NaCl treatment induced a significant ($p<0.05$) increase in *SbNHX2* expression, in comparison with the NaCl treatment alone (Fig. 7b).

The *SbHKT1* expression was generally lower than that of *SbNHX2* in both roots and shoots of both genotypes at days 6 and 10 (Fig. S5c-d and Fig. 7c-d in comparison). Furthermore, the expression of *SbHKT1* gene increased in the roots of both genotypes at day 10 in comparison with day 6 (Fig. 7c-d and Fig. S5c-d in comparison). The highest *SbHKT1* transcript abundance was detected in the roots of 10-day-old Bianca seedlings under P and P+NaCl treatments (Fig. 7c), whereas no significant differences among treatments were detected in Tonkawa roots at the same time point (Fig. 7d). However, *SbHKT1* expression increased in the roots of 10-day-old Tonkawa seedlings compared with those of 6-days-old seedlings (Fig. 7d and Fig. S5d). After 10 days, *SbHKT1* transcript levels remained negligible in the shoots of both genotypes (Fig. 7c-d).

Overall, seed priming with 24-eBL differentially modulated *SbNHX2* expression in roots and shoots of the two genotypes and, interestingly, increased the gene expression in Tonkawa roots under salt stress.

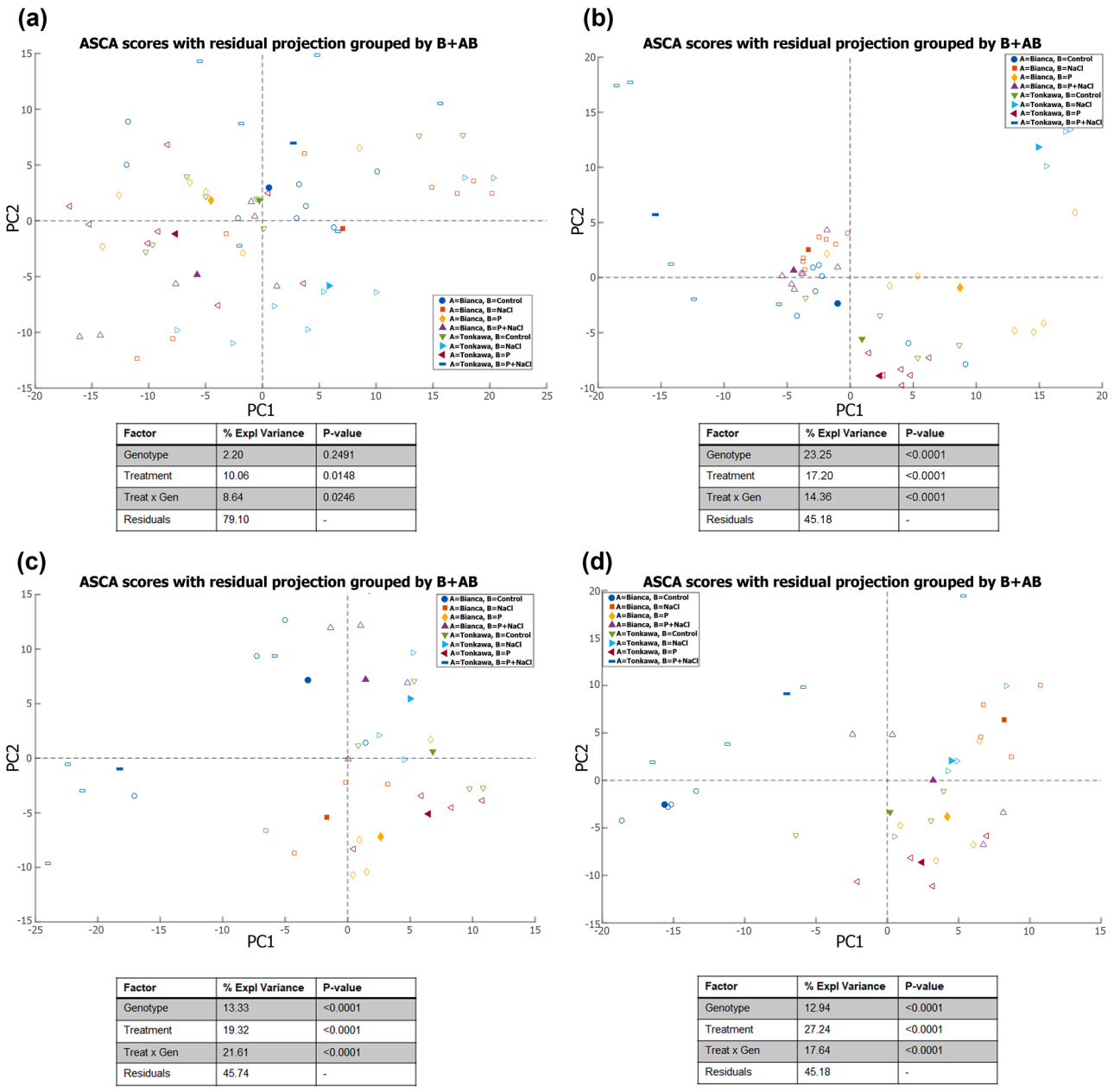


| Factor | % Expl Variance | P-value |
|---|---|---|
| Genotype | 2.20 | 0.2491 |
| Treatment | 10.06 | 0.0148 |
| Treat x Gen | 8.64 | 0.0246 |
| Residuals | 79.10 | - |

| Factor | % Expl Variance | P-value |
|---|---|---|
| Genotype | 23.25 | <0.0001 |
| Treatment | 17.20 | <0.0001 |
| Treat x Gen | 14.36 | <0.0001 |
| Residuals | 45.18 | - |

| Factor | % Expl Variance | P-value |
|---|---|---|
| Genotype | 13.33 | <0.0001 |
| Treatment | 19.32 | <0.0001 |
| Treat x Gen | 21.61 | <0.0001 |
| Residuals | 45.74 | - |

| Factor | % Expl Variance | P-value |
|---|---|---|
| Genotype | 12.94 | <0.0001 |
| Treatment | 27.24 | <0.0001 |
| Treat x Gen | 17.64 | <0.0001 |
| Residuals | 45.18 | - |

**Fig. 6.** ANOVA-Simultaneous Component Analysis (ASCA) of Raman spectra acquired from sorghum roots subjected to different treatments. (a–d) Score plots of the first two principal components (PC1 and PC2) obtained from PCA of the combined treatment and treatment × genotype effect matrices for the different root regions: (a) adventitious meristem (ARM); (b) lateral root meristem (LRM); (c) differentiated region epidermis (E); (d) differentiated region cortex (C). Spectra were collected on adventitious roots of 10 days old seedlings non-primed and not exposed to NaCl (Control), non-primed and exposed to 150 mM NaCl (NaCl), primed only (P) and primed and exposed to NaCl (P + NaCl). To facilitate visualization of the overall model structure, residual variation not explained by the investigated effects was back-projected onto the score space.

Moreover, seed priming differentially affected *SbHKT1* expression between the two organs and genotypes. In fact, it increased *SbHKT1* transcript abundance in the roots, but not in the shoots, of both genotypes, although this effect was significant in the salt-tolerant Bianca.

### *3.6. 24-eBL seed priming limits $Na^+$ translocation to the aerial organs without affecting $K^+$ homeostasis*

To assess the $Na^+$ accumulation in roots and its translocation to the shoot, the $Na^+$ content was quantified in both organs of Bianca and Tonkawa at 6 and 10 days after sowing. In addition, $K^+$ content was quantified to assess whether salt stress disrupted $Na^+/K^+$ homeostasis and whether the 24-eBL seed priming affected this response, given the key role of $K^+$ in maintaining osmotic balance and regulating ion transport across cell membranes (Mostofa et al., 2022).

Six days after sowing, $Na^+$ content was higher in the roots than in the shoots in the seedlings of both Bianca and Tonkawa exposed to NaCl or to P+NaCl treatments (Fig. S6a-b). However, in Tonkawa the difference in $Na^+$ content between roots and shoots was minimal, suggesting a higher $Na^+$ translocation to the shoots in this genotype in comparison with Bianca. The P+NaCl treatment slightly increased the $Na^+$ content in the roots and decreased it in the shoots, although these changes were not significant (Fig. S6a-b).

At day 10, the $Na^+$ accumulation increased in Bianca roots under NaCl and P+NaCl, whereas shoot $Na^+$ levels remained similar to that observed at day 6 (Fig. 8a and Fig S6a in comparison). The P+NaCl

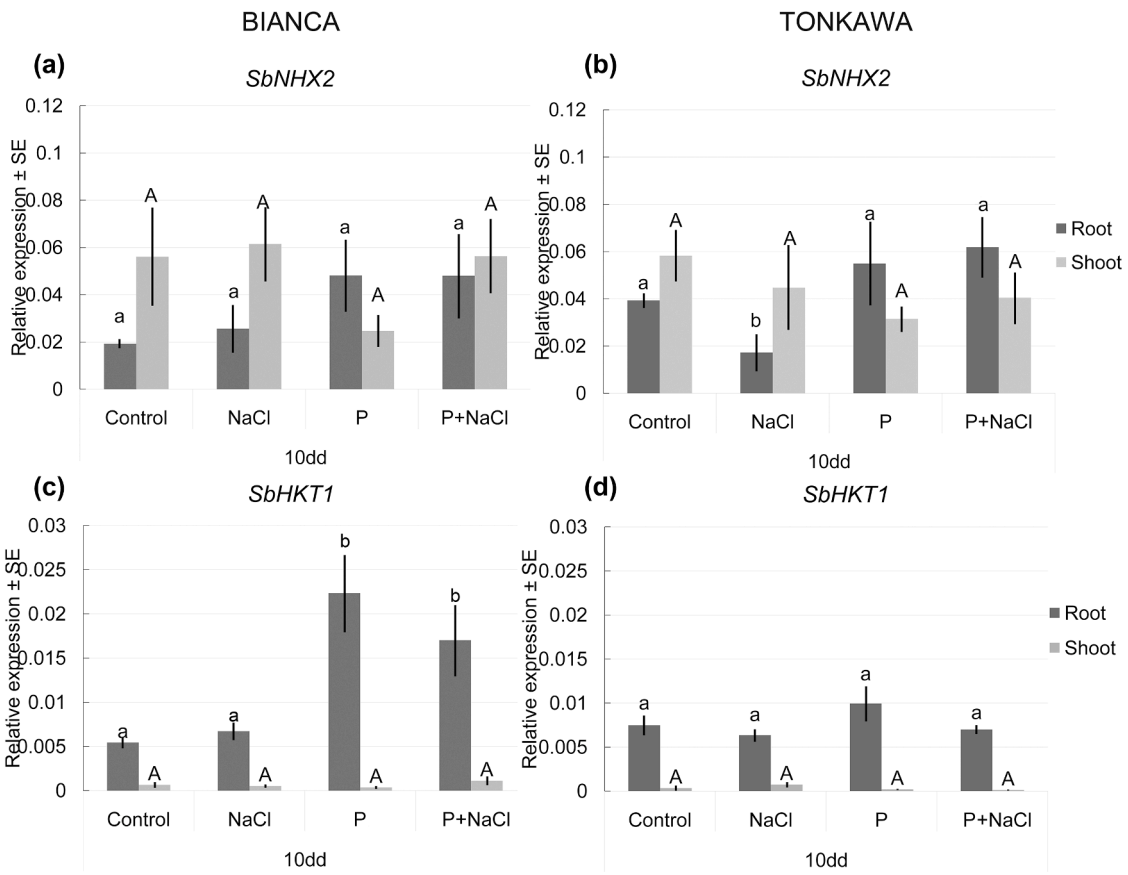


**Fig. 7.** Relative expression of *SbNHX2* (main vacuolar $Na^+$ transporter) (a,b) and *SbHKT1* (main cell membrane $Na^+$ and $K^+$ transporter) (c,d) in the shoots and roots of 10-day-old Bianca and Tonkawa seedlings non-primed and not exposed to NaCl (Control), non-primed and exposed to 150 mM NaCl (NaCl), primed only (P) and primed and exposed to NaCl (P+NaCl). Transcript abundance was normalized to *SbUBQ*. Different lowercase letters indicate significant differences among treatments in roots, while different uppercase letters indicate significant differences among treatments in shoots for at least $p<0.05$. The same letter shows no significant difference within the same genotype and organ. **N=9.**

treatment significantly ($p<0.05$) enhanced the difference between roots and shoots compared to NaCl alone, indicating greater $Na^+$ retention in roots and reduced translocation to shoots.

At day 10, in Tonkawa seedlings exposed to NaCl or to P+NaCl, the root $Na^+$ accumulation was higher than at day 6 (Fig. 8b and Fig. S6b in comparison). Furthermore, P+NaCl treatment significantly ($p<0.05$) reduced shoot $Na^+$ content and increased this ion accumulation in the roots compared with the salt alone treatment (Fig. 8b), indicating a positive effect of seed priming in limiting $Na^+$ translocation to the shoots also in this genotype.

Overall, the seed priming increased $Na^+$ accumulation in roots and limited its translocation to the shoot in both genotypes.

At 6 days after sowing, the amount of $K^+$ in the roots and in the shoots of Control seedlings was similar in Bianca and Tonkawa and, as expected, was much higher than $Na^+$ content (Fig. S6a-b). Seed priming alone did not affect $K^+$ accumulation and translocation in both genotypes, while NaCl significantly reduced the $K^+$ content in both shoots ($p<0.001$) and roots ($p<0.0001$) (Fig. S6a-b). The P+NaCl treatment resulted in $K^+$ levels comparable to those observed under salt treatment alone in both genotypes and organs (Fig. S6a-b).

At day10, Control and P-treated Tonkawa and Bianca seedlings showed higher $K^+$ content in the roots than in the shoots (Fig. 8c-d). Salt treatment significantly reduced $K^+$ levels in both organs of both genotypes, particularly in the roots. Ultimately, in both genotypes and organs, the P+NaCl treatment resulted in a $K^+$ content similar to that measured under NaCl alone (Fig. 8c-d).

Overall, these results indicate that NaCl exposure induced increased $Na^+$ accumulation predominantly in roots than in shoots, and this effect was further enhanced by the P+NaCl treatment, particularly in Tonkawa. The NaCl treatment, either alone or following by 24-eBL priming, resulted in a similar reduction in roots and shoots $K^+$ levels in both genotypes, in comparison with Control conditions.

### *3.7. 24-eBL seed priming increases $Na^+$ vacuole sequestration in a genotype- and cell type-dependent manner*

Given the higher $Na^+$ levels detected in the roots, we investigated whether the 24-eBL seed priming affected the $Na^+$ vacuolar compartmentalization in this organ. Adventitious roots of 10-day-old seedlings, grown under Control, NaCl and P+NaCl treatments, were co-stained with the $Na^+$-sensitive fluorescent dye CoroNa Green and the cell membranes probe FM 4-64. CoroNa Green fluorescence was used to visualize intracellular $Na^+$ distribution, and sodium ion levels were quantified based on the intensity of the green fluorescence signal. FM4-64 staining was used to label the cellular membranes and distinguish cytoplasmic from vacuolar regions, allowing the relative $Na^+$-associated fluorescence signal in the two compartments to be evaluated (Fig. S3a-f).

Meristematic cells in the AR apex and the cortical parenchyma cells in the differentiated (mature) region of ARs were analysed. Meristematic cells of Control ARs showed a similarly low $Na^+$ fluorescence signal in cytoplasm and vacuoles in both genotypes (Fig. 9a-b, g-h). In the root meristematic cells of Bianca, NaCl treatment resulted in a significantly ($p<0.001$) higher $Na^+$ signal in the cytoplasm than in the vacuoles (Fig. 9c,g). In contrast, under P+NaCl treatment the $Na^+$ signal was significantly ($p<0.001$) higher in the vacuoles than in the cytoplasm (Fig. 9e and Inset, g). The meristematic cells of Tonkawa ARs showed a

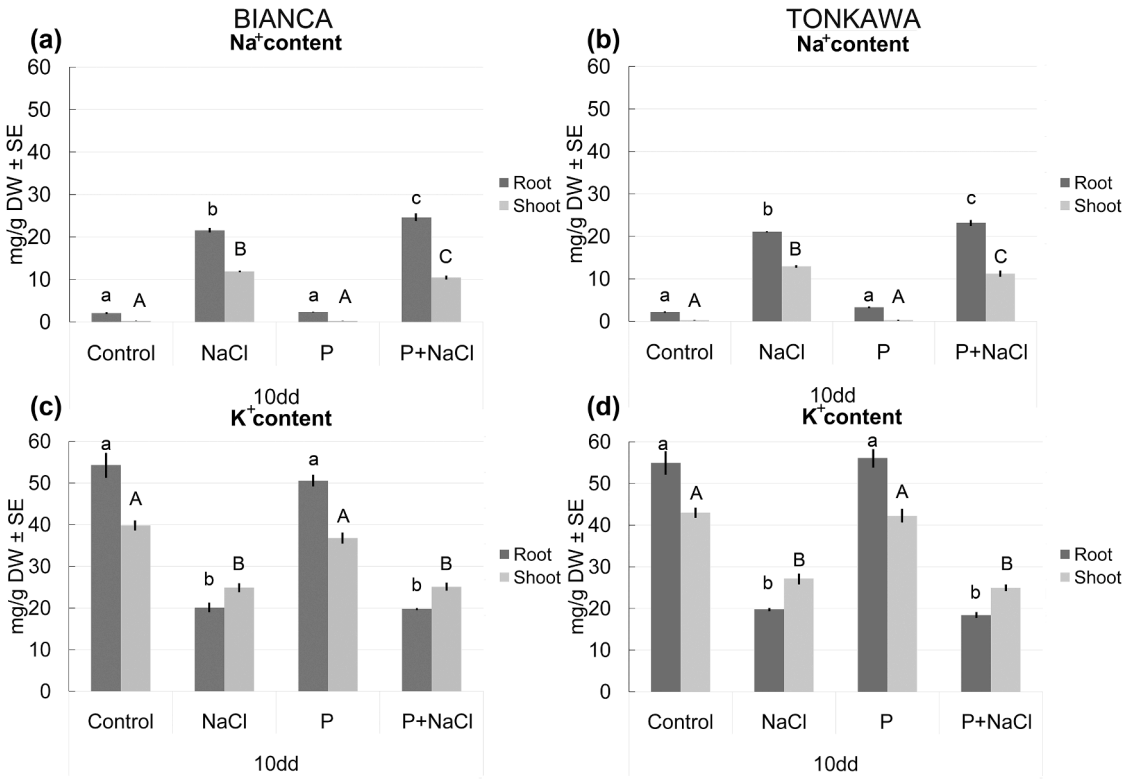


**Fig. 8.** Mean content of $Na^+$ (a,b) and $K^+$(c,d), in shoots and roots of 10-day-old Bianca and Tonkawa seedlings not exposed (Control) or exposed to 150 mM NaCl (NaCl), or treated with 1μM 24-eBL seed priming (P), or with 1μM 24-eBL seed priming followed by 150 mM NaCl (P+NaCl). Different lowercase letters indicate significant differences among treatments in roots, while different uppercase letters indicate significant differences among treatments in shoots for at least $p<0.05$. The same letter shows no significant difference within the same genotype and organ. N=3.

cytoplasmic $Na^+$ signal significantly ($p<0.001$) higher than the vacuolar signal under both NaCl and P+NaCl treatments (Fig. 9d,f,h).

In the cortical cells of the mature region of Control ARs, both Bianca and Tonkawa seedlings, showed a similarly low $Na^+$ signal in both the cytoplasm and the vacuole (Fig. 9i-j, o-p). In Bianca cortical cells exposed to either NaCl or P+NaCl treatments, the vacuolar $Na^+$ signal was significantly ($p<0.001$) higher than the cytoplasmic signal (Fig. 9k, m,o). Interestingly, in the cortical cells of the mature root zone of Tonkawa, a significant increase ($p<0.0001$) in the vacuolar $Na^+$ signal was observed only following P+NaCl treatment in comparison with NaCl treatment alone (Fig. 9l,n,p).

Overall, these results highlight a cell type- and genotype-dependent different ability in $Na^+$ compartmentalization. Bianca exhibited a greater capacity for $Na^+$ vacuolar sequestration than Tonkawa under NaCl stress. In Bianca differentiated (mature) cells accumulated $Na^+$ in the vacuole irrespective of seed priming, whereas meristematic cells showed vacuolar $Na^+$ accumulation only after seed priming. In Tonkawa, vacuolar $Na^+$ accumulation occurred only in the differentiated cells following seed priming. By contrast, in the meristematic cells, $Na^+$ remained predominantly cytoplasmic also after 24-eBL seed priming treatment.

## 4. Discussion

In the present study, we showed that 24-eBL seed priming improved post-embryonic root system development in Tonkawa, a salt-sensitive sorghum genotype, under salt stress, whereas its effects were limited in Bianca, a genotype known for its salt tolerance. Our results indicate that 24-eBL seed priming triggers a range of responses, from biochemical modifications in root cell wall- and membrane-associated components to the modulation of genes encoding $Na^+$ and $K^+$ transporters. All these processes were associated with changes in BR-perception, which are detectable in the roots within the first few days after seed germination, and became firmly established by day 10. Overall, our results suggest that these changes may contribute to the ability of Tonkawa's root system to sustain plant growth and development under severe stress conditions, such as salinity.

### *4.1. Seeds primed with 24-eBL produce seedlings with improved root adaptation to salt stress in a salt-sensitive sorghum genotype through a direct effect on cell membranes stabilization*

Root system architecture plasticity plays a critical role in crop adaptation to abiotic stresses such as salinity. In sorghum, the primary root (PR) is the first root to emerge and develops from the embryonic radicle. Soon after the PR elongation begins the seminal roots start to emerge from the embryonic region above the PR. The PR is relatively short-lived as its function is progressively taken over by the adventitious roots (ARs) that develop from the culm nodes (Singh et al., 2010). Consistent with their embryonic origin, the present data shows that PRs are relatively unaffected by salt stress, apart from a developmental delay in the sensitive genotype, which was not rescued by 24-eBL seed priming (P+NaCl treatment). By contrast, salt stress significantly affected the number and development of ARs and their associated lateral roots (LRs) in both genotypes, with a stronger impact in Tonkawa. Interestingly, the brassinosteroid seed priming promoted AR formation at 6 days after sowing in seedlings of both genotypes, but particularly in Tonkawa, where the effect was more pronounced than in Bianca. These results are consistent with previous findings in the aerial organs of older plants of the same sorghum genotype, in which 24-eBL seed priming alleviated the salt-induced alterations in leaf anatomy and restored photosynthetic efficiency in Tonkawa plants grown in pots under saline conditions for approximately two months (Peduzzi et al., 2025). In the present study, we show that the beneficial effects of the BR seed priming become

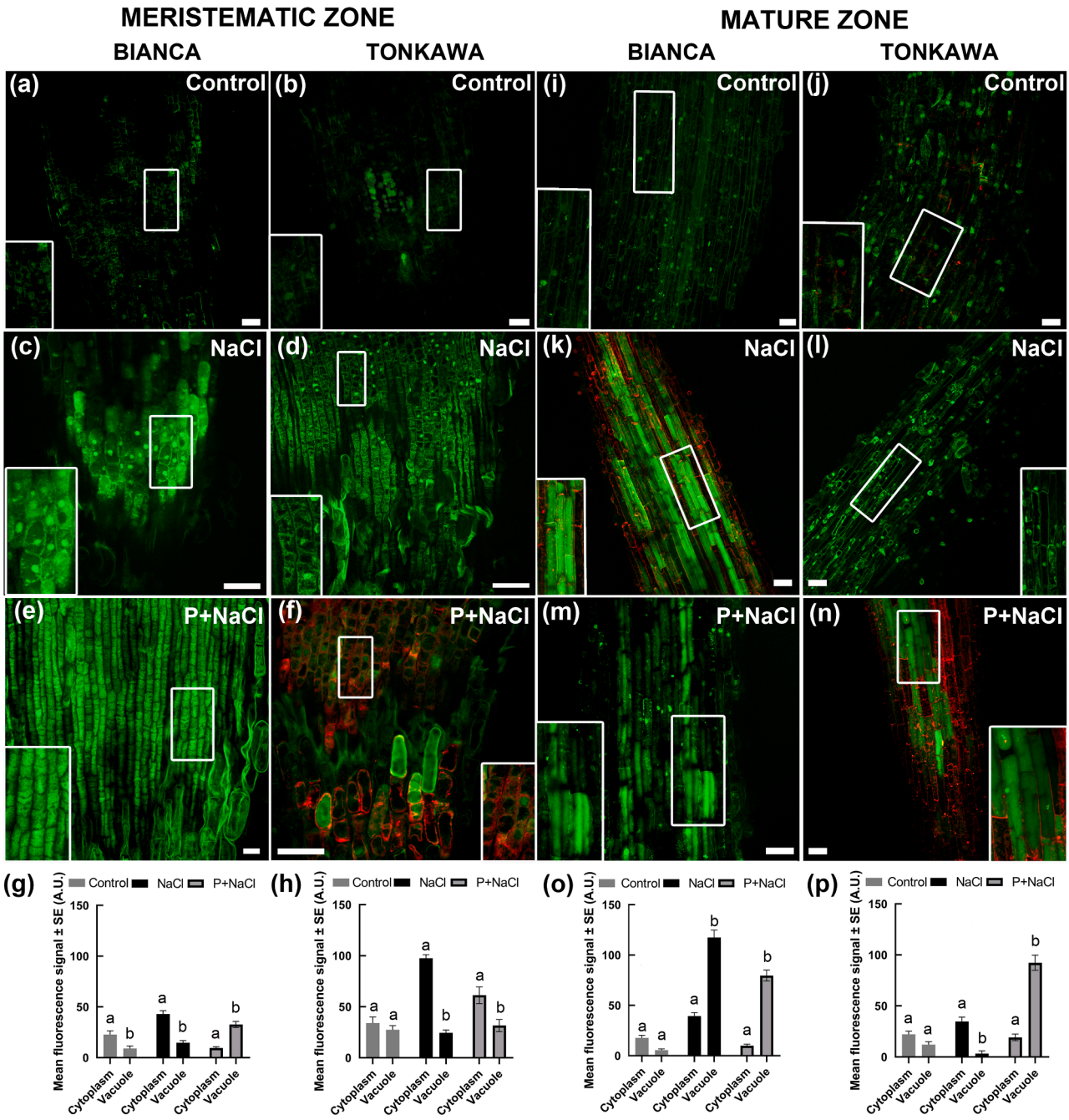


**Fig. 9.** Representative merged confocal images showing the intracellular distribution of $Na^+$-associated fluorescence in the meristematic (a–f) and differentiated cortical (i–n) regions of adventitious roots co-stained with the $Na^+$-sensitive probe CoroNa Green AM and the membrane-selective probe FM4-64. Images were acquired on ARs of 10-day-old Bianca (a,c,e,i,k,m) and Tonkawa (b,d,f,j,l,n) seedlings non-primed and not exposed to NaCl (Control; a-b,i-j), non-primed and exposed to 150 mM NaCl (NaCl; c-d, k-l) and primed and exposed to NaCl (P+NaCl; (e-f, m-n), Graphs show the mean CoroNa Green fluorescence signal (±SE) in arbitrary units (AUs) in AR cells of Bianca (g, o) and Tonkawa (h, p) meristematic zone (g-h) or mature zone (o-p). Insets show magnified views of the regions selected for fluorescence quantification analysis. Different letters represent statistically significant differences among cellular compartments and treatments within the same root region at least for $p<0.05$. The same letter shows no significant difference within the same root region. N=45. Bars= 20 μm (a,b,e), 50 μm (c,d,f,i,j,k,l,m,n).

evident in the root system within the first few days after germination. Since water and nutrients are absorbed by the roots and translocated to the shoots, root system architecture and root growth directly influence leaf functionality and are major determinants of crop yield (Brown and Scott, 1984). This is particularly relevant in cereals, like sorghum, whose mature root system is composed by many ARs and LRs arising from them. In accordance, our previous results showed that the salt-tolerant genotype, Bianca, was characterized by an intrinsic ability to establish a well-developed root system (Peduzzi et al., 2024). The present findings highlight that, in the salt-sensitive genotype Tonkawa, 24-eBL seed priming improves the formation of both ARs and lateral root primordia (LRPs), as well as ARs growth under salt stress. It has been demonstrated in Arabidopsis that salt stress initially inhibits root growth and elongation (Geng et al., 2013). This initial phase may last for several days, and the subsequent recovery of the root growth appears to be mediated by BRs signalling, demonstrating that this pathway contributes to the restoration of root growth altered by salt stress in Arabidopsis (Geng et al., 2013). Indeed, Geng and co-workers (2013) reported that the

Arabidopsis *bzr1-D* gain-of-function mutant, carrying a mutation in *BZR1*, a positive regulator of brassinosteroid-induced growth, and the *bri1-5* mutant, carrying a weak allele of *BRI1* and showing reduced BR signalling, exhibited contrasting responses to salt exposure. Specifically, after salt exposure, *bzr1-D*, exhibited a substantial reduction in the initial growth inhibition phase compared with the wild type (Wang et al., 2002). On the contrary, the *bri1-5* mutant showed a prolonged root growth inhibition phase (Noguchi et al., 1999). These observations indicate that the re-establishment of BR signalling contributes to the timing and extent of root growth recovery after salt exposure (Geng et al., 2013). Therefore, it is possible that, an enhanced BR signalling, resulting from the increased *SbBRI1* expression, induced by the priming treatment in the roots of the salt-sensitive sorghum genotype here used, might contribute to an overall improvement in root system growth. Consistent with this hypothesis, our results show that P+NaCl treatment enhances ARs growth and significantly increases LRPs density in the salt-sensitive genotype. In Arabidopsis, the periodic specification of lateral root pre-branch sites along the primary root is controlled by an oscillatory developmental mechanism known as the "root clock" (Moreno-Risueno et al., 2010). Modelling studies have reported that the frequency of LR formation results from the interaction between root meristem size and growth, and auxin movement along the root toward its apex (van den Berg et al., 2021). Since BR signalling regulates both the shape and growth of the root meristem (Fridman et al., 2021), these phytohormones may also play a broader role in regulating overall root architecture, as recently suggested by Khandal and co-workers (2025). Based on our results and on those reported in the literature, we hypothesize that BRs play a positive role in modulating root system architecture thereby increasing salt tolerance in the salt-sensitive sorghum even, and perhaps mainly, when applied as a seed priming treatment.

Our micro-spectroscopic analysis revealed a marked reduction in the Raman band at 1450 $cm^{-1}$ in cells of both adventitious root meristem (ARM) and lateral root meristem (LRM) of Tonkawa under salt treatment, revealing alterations in aliphatic cellular components, including membrane lipids and proteins. In contrast, NaCl treatment induced a strong increase in the same Raman band in Bianca ARM and LRM cells. Given that this band is associated with $CH_2/CH_3$ deformation vibrations, its decrease, in the salt-sensitive genotype, may reflect strong salt-induced membrane disorganization and protein modifications in this genotype. These changes may be related to osmotic and oxidative stress, which are known to promote lipid peroxidation and impair cellular integrity under salinity (Guo et al., 2019, and references therein). Conversely, the increased signal observed in the salt-tolerant genotype may indicate a different pattern of remodelling or maintenance of lipid- and protein-associated components, potentially contributing to its greater ability to preserve cellular integrity under salt stress. Consistent with the nature of meristematic cells, which possess poorly developed primary cell walls, only minor variations were observed in the Raman bands at 882 and 1050 $cm^{-1}$, commonly associated with skeletal vibrations of cellulose-type polysaccharides, even after salt stress exposure in both genotypes. Furthermore, increased intensities of the Raman bands at 1050 and 1730 $cm^{-1}$ in differentiated epidermal and cortical cells under salt stress were observed, particularly in Tonkawa roots. These variations suggest substantial modifications in cell-wall polysaccharides and esterified wall components. In contrast, in the same cells, the Raman signal at 1450 $cm^{-1}$, coherent with membrane lipids and proteins, showed only a slight increase under salt stress compared with the Control. Interestingly, the application of BRs, as a seed priming agent, restored all Raman bands to levels comparable to those of the unstressed Control, suggesting that priming counteracted, at least in part, the salt-induced biochemical remodelling in differentiated root cells.

Under our experimental conditions, the enhanced salt tolerance induced by BR in Tonkawa may be linked with an improved preservation of membrane-associated cellular components in both meristematic and differentiated cells. This interpretation is supported by the lower malondialdehyde (MDA) levels observed under P+NaCl treatment compared with NaCl treatment alone, as well as by the likely indirect effect of seed priming on cell wall structure, as highlighted by Raman analyses and consistent with previous reports (Guo et al., 2019, and references therein; Basit et al., 2021). In fact, reduced membrane damage may in turn decrease the need for a cellulose-reinforced wall to counteract salt toxicity. Furthermore, the ASCA analysis demonstrated that the genotype x treatment interaction effect was particularly pronounced in the differentiated tissues in comparison with the meristematic tissues, indicating that the impact of priming on the response to salinity is tissue-dependent and differs between the two genotypes.

Salt stress severely compromises root development by inducing oxidative stress, characterized by excessive accumulation of ROS capable of altering numerous cellular components such as membrane lipids, proteins, and DNA in different plant species including sorghum (Zhang et al., 2014; Ahmad et al., 2019; Peduzzi et al., 2024). Among the ROS, $H_2O_2$ and $O_2^-$ are the main responsible in lipid peroxidation, which damage cell membranes and increase MDA levels (Denhavi et al., 2024). Our results showed that the salt treatment significantly increased the MDA levels in Tonkawa, whereas the 24-eBL seed priming significantly decreased them, particularly in roots, thereby suggesting an attenuation of salt-induced oxidative damages in the sensitive genotype. In Bianca no significant difference in MDA levels was observed between the Control and NaCl treated seedlings, in accordance, with the low lipid peroxidation reported in other tolerant sorghum genotypes, after salt exposure (Denhavi et al., 2024). Nevertheless, under salt stress, the 24-eBL priming reduced lipid peroxidation in both genotypes. A similar effect was also reported in rice seedlings exposed to chromium, in which seed priming with 0.01 μM 24-eBL protected cells from membrane damages by reducing ROS activity and, consequently, MDA content (Basit et al., 2021). Indeed, BRs are well known to modulate the activity of both enzymatic and non-enzymatic components of the antioxidant defence system in abiotic stressed plants (Vardhini and Anjum, 2015). Present data are therefore consistent with the beneficial role of BRs in regulating the antioxidant response of sorghum, even when supplied as seed priming agents, and, also, in promoting an overall rebalancing of root system growth under saline conditions. Moreover, the reduction of MDA levels under salt stress may also be attributed to improved ionic homeostasis. In particular, enhanced $Na^+$ vacuolar compartmentalization in differentiated root cells, as observed in the present study and previously reported as a mechanism underlying BR-mediated salt tolerance (Anwar et al., 2018; Tanveer et al., 2018), may have contributed to limiting oxidative membrane damage.

Overall, our results support a greater response of the salt-sensitive genotype to BR seed priming which may be associated with the stronger alteration of root development under salt stress. Indeed, root system architecture is highly plastic and can be extensively remodeled in response to salinity, representing an important component of plant adaptation to changing environmental conditions (Tariq et al., 2026). In our conditions, Bianca was better able to maintain root growth under salt stress, whereas Tonkawa showed more pronounced alterations in root development. The stronger response to BR treatment in Tonkawa may therefore reflect the ability of BRs to counteract stress-induced changes in root development, promoting ARs and LRs formation and elongation and thereby contributing to the restoration of root system function. This interpretation is consistent with recent evidence showing that BR- and auxin-related signaling through TaGSK3 regulates lateral root developmental plasticity in wheat under salt stress, thereby facilitating root recovery following stress relief (Zhang et al., 2026). Thus, the greater benefit of BR-based seed priming in Tonkawa may not reflect a greater intrinsic sensitivity to BRs, but rather a greater potential for BR-mediated recovery of root development under salt stress.

### 4.2. 24-eBL seed priming enhances salt tolerance in the sensitive genotype by modulating cell type-specific $Na^+$ management through an increased expression of *SbNHX2*

In this study, we observed that both genotypes predominantly accumulate $Na^+$ ions in the roots of the NaCl-treated seedlings, and that 24-eBL seed priming further enhances this ability. However, the tolerant genotype, Bianca, exhibited a more efficient mechanism of sodium ions management. Confocal analysis highlighted the remarkable ability of this genotype to sequester $Na^+$ within the vacuoles of differentiated root cells, in contrast to the sensitive Tonkawa, which accumulated $Na^+$ predominantly in the cytoplasm of the same cell types. Thus, a greater capacity for vacuolar $Na^+$ sequestration may represent a trait associated with salt stress tolerance, especially since a similar pattern was previously observed in Della, another salt-tolerant sorghum genotype (Abuslima et al., 2022). As here reported, in the mature root region of Bianca seedlings, $Na^+$ was sequestered in the vacuoles, and the seed priming did not affect this mechanism. On the contrary, meristematic cells of the ARs exhibited predominantly cytoplasmic $Na^+$ accumulation, under salt stress, whereas BR-priming increased the vacuolar $Na^+$ sequestration. This response may be attributed to the increased expression of the *SbBR1* gene in roots of the same age following seed priming treatment, which could promote early activation of vacuolar transporters in undifferentiated cells. Consistently, BR signalling is known to play a positive role in regulating vacuolar morphology and size in meristematic cells of Arabidopsis (Yamagami et al., 2018), while salt stress can induce vacuolar fragmentation in the same cells (Liu et al., 2025). It is therefore possible that the combined action of the inherent tolerance of Bianca and the precocious formation of regular vacuoles in the meristematic cells due to the 24-eBL priming contributes to the enhanced vacuolar sequestration of the $Na^+$ ion in these cells. In contrast, in the root meristematic cells of Tonkawa, 24-eBL seed priming did not increase vacuolar $Na^+$ accumulation, suggesting that, in the salt-sensitive genotype, BR priming fails to restore vacuolar integrity and/or the expression of vacuolar transporters to levels required for effective $Na^+$ sequestration into the vacuoles of meristematic cells. Accordingly, the ASCA analysis demonstrated that 24-eBL seed priming-related biochemical changes in Raman spectra were less pronounced in the root meristematic cells of Tonkawa than in differentiated epidermal and cortical cells.

In this regard, we suggest that the improved root response to salinity induced by 24-eBL seed priming in Tonkawa may be mainly attributed to an increased vacuolar $Na^+$ compartmentalization in the differentiated root cells. This response may promote $Na^+$ detoxification, thereby supporting cellular and organ functionality under salt stress. Indeed, this spatial regulation of $Na^+$ handling is consistent with the observed reduction in membrane damage and the improved post-embryonic root system development observed in primed Tonkawa seedlings. More broadly, our results suggest that BR-mediated priming may enhance salt tolerance through the coordinated modulation of root development, oxidative stress, and ion homeostasis. The stimulation of root branching, reduced MDA accumulation, and modulation of ion transport gene expression may collectively contribute to maintaining root functionality, limiting oxidative damage, and improving $Na^+$ uptake, transport, and/or sequestration. These responses are consistent with previous evidence showing that exogenous BRs can simultaneously promote root growth, enhance antioxidant responses, and improve ion homeostasis under salt stress (Wang et al., 2023b).

Although the present dataset does not allow direct correlations or causal relationships among these parameters to be established, their concomitant modulation supports the hypothesis that BR seed priming promotes salt tolerance through the coordinated regulation of root development, oxidative stress, and ion homeostasis.

## 5. Conclusions

Brassinosteroids (BRs) are increasingly recognized as powerful natural regulators of plant growth and stress adaptation, with considerable potential for improving crop performance under adverse environmental conditions. In this regard, seed priming represents an attractive and practical approach, as it can be easily applied on a large scale and may provide long-lasting benefits throughout plant development.

Our findings provide new insights into the role of BR signalling during the early stages of sorghum growth and, in particular, into their contribution to root responses to salinity. Both sorghum genotypes predominantly accumulate sodium in the roots, where the effects of 24-eBL seed priming were evident. Importantly, this study demonstrates that BR seed priming can enhance salt tolerance in sensitive Tonkawa genotype by reinforcing BR signalling and activating key physiological and molecular mechanisms involved in ion homeostasis and stress adaptation, such as reduction of the oxidative stress and increase of sodium ion vacuolar sequestration, through the activation of genes encoding vacuolar transporters. The responses to 24-eBL seed priming were strongly genotype- and cell type-dependent. While the salt-tolerant Bianca displayed an intrinsic capacity for efficient $Na^+$ management, the sensitive Tonkawa showed a greater potential for improvement following seed priming. This finding suggests that the effectiveness of BR priming may depend not only on the intrinsic sensitivity of a genotype to hormone, but also on its capacity to modulate root development and stress-adaptative responses under salinity.

Taken together, our results support BR seed priming as a promising strategy to enhance sorghum performance under saline conditions. More broadly, they highlight the importance of early root responses and cell type-specific regulation of ion homeostasis in plant adaptation to salinity and provide a basis for further investigation of the molecular mechanisms underlying BR-mediated stress tolerance.

## CRediT authorship contribution statement

**A. Peduzzi:** Writing – original draft, Methodology, Investigation, Funding acquisition, Data curation, Conceptualization. **D. Piacentini:** Writing – review & editing, Methodology, Data curation. **S. D'Angeli:** Methodology, Data curation. **F. Sciubba:** Methodology. **F. Marini:** Validation, Methodology, Data curation. **T. Napoleoni:** Methodology. **E. Speranza:** Methodology. **E. Eiche:** Methodology, Data curation. **M. Riemann:** Writing – review & editing. **P. Nick:** Writing – review & editing, Methodology. **M.M. Altamura:** Writing – review & editing. **G. Falasca:** Writing – review & editing, Writing – original draft, Validation, Supervision, Methodology, Funding acquisition, Data curation, Conceptualization.

## Declaration of competing interest

The authors declare that they have no known competing financial interests or personal relationships that could have appeared to influence the work reported in this paper.

## Acknowledgements

The Authors thank Padana Sementi Elette S.r.l for providing the seeds of Bianca and Tonkawa genotypes, Dr Nitin Pawar for his guidance during the qRT-PCR analyses and Dr Chantalle Kotschenreuther for her technical assistance with ICP-OES data collection.

## Supplementary materials

Supplementary material associated with this article can be found, in the online version, at doi:10.1016/j.stress.2026.101539.

## Data availability

Data will be made available on request.

## References


Abdalla, M., Ahmed, M.A., Cai, G., Zarebanadkauki, M., Carminati, A., 2022. Coupled effects of soil drying and salinity on soil–plant hydraulics. Plant Physiol. 190, 1228–1241. https://doi.org/10.1093/plphys/kiac229.

Abuslima, E., Kanbar, A., Raorane, M.L., Eiche, E., Junker, B.H., Hause, B., Riemann, M., Nick, P., 2022. Gain time to adapt: how sorghum acquires tolerance to salinity. Front. Plant Sci. 13. https://doi.org/10.3389/fpls.2022.1008172.

Ahmad, P., Tripathi, D.K., Deshmukh, R., Pratap Singh, V., Corpas, F.J., 2019. Revisiting the role of ROS and RNS in plants under changing environment. Environ. Exp. Bot. 161, 1–3. https://doi.org/10.1016/j.envexpbot.2019.02.017.

Ahanger, M.A., Ashraf, M., Bajguz, A., Ahmad, P., 2018. Brassinosteroids regulate growth in plants under stressful environments and crosstalk with other potential phytohormones. J. Plant Growth Regul. 37, 1007–1024. https://doi.org/10.1007/s00344-018-9855-2.

Allahverdian, M., Rahmani, F., 2025. Epibrassinolide seed priming alleviates alkaline stress by enhancing antioxidant defense in dragonhead plants. Sci. Rep. 16, 1137. https://doi.org/10.1038/s41598-025-30763-2.

Anwar, A., Liu, Y., Dong, R., Bai, L., Yu, X., Li, Y., 2018. The physiological and molecular mechanism of brassinosteroid in response to stress: a review. Biol. Res. 51, 46. https://doi.org/10.1186/s40659-018-0195-2.

Barnes, R.J., Dhanoa, M.S., Lister, S.J., 1989. Standard normal variate transformation and de-trending of near-infrared diffuse reflectance spectra. Appl. Spectrosc. 43, 772–777. https://doi.org/10.1366/0003702894202201.

Basit, F., Chen, M., Ahmed, T., Shahid, M., Noman, M., Liu, J., An, J., Hashem, A., Fahad Al-Arjani, A-B, Alqarawi, A.A., Alsyed, M.F.S., Abd-Allah, E.F., Hu, J., Guan, Y., 2021. Seed priming with brassinosteroids alleviates chromium stress in rice cultivars via improving ROS metabolism and antioxidant defense response at biochemical and molecular levels. Antioxidants 10, 1089. https://doi.org/10.3390/antiox10071089.

Brown, D.A., Scott, H.D., 1984. Dependence of crop growth and yield on root development and activity. In: Barber, S.A., Bouldin, D.R. (Eds.), Roots, Nutrient and Water Influx, and Plant Growth. https://doi.org/10.2134/asaspecpub49.c6.

Chawla, S., Jain, S., Jain, V., 2013. Salinity induced oxidative stress and antioxidant system in salt-tolerant and salt-sensitive cultivars of rice (*Oryza sativa* L.). J. Plant Biochem. Biotechnol. 22, 27–34. https://doi.org/10.1007/s13562-012-0107-4.

Clark, K.R., Goldberg Oppenheimer, P., 2024. Vibrational spectroscopic profiling of biomolecular interactions between oak powdery mildew and oak leaves. Soft Matter 20, 959–970. https://doi.org/10.1039/d3sm01392h.

Conrath, U., Beckers, G.J.M., Langenbach, C.J.G., Jaskiewicz, M.R., 2015. Priming for enhanced defense. Annu. Rev. Phytopathol. 53, 97–119. https://doi.org/10.1146/annurev-phyto-080614-120132.

Cui, F., Liu, L., Zhao, Q., Zhang, Z., Li, Q., Lin, B., Wu, Y., Tan, S., Xie, Q., 2012. Arabidopsis ubiquitin conjugase UBC32 is an ERAD component that functions in brassinosteroid-mediated salt stress tolerance. Plant Cell 24, 233–244. https://doi.org/10.1105/tpc.111.093062.

Dehnavi, A.R., Zahedi, M., Piernik, A., 2024. Understanding salinity stress responses in sorghum: exploring genotype variability and salt tolerance mechanisms. Front. Plant Sci. 14. https://doi.org/10.3389/fpls.2023.1296286.

Della Rovere, F., Anupama Fernando Malimage, S., D'Angeli, S., Peduzzi, A., Piacentini, D., Altamura, M.M., Falasca, G., 2025. Brassinosteroids and jasmonates mitigate arsenite- and arsenate-induced morpho-anatomical anomalies in Arabidopsis roots. Plant Sci. 359, 112625. https://doi.org/10.1016/j.plantsci.2025.112625.

Fracasso, A., Magnanini, E., Marocco, A., Amaducci, S., 2017. Real-Time determination of photosynthesis, transpiration, water-use efficiency and gene expression of two *Sorghum bicolor* (Moench) genotypes subjected to dry-down. Front. Plant Sci. 8. https://doi.org/10.3389/fpls.2017.00932.

Fridman, Y., Strauss, S., Horev, G., Ackerman-Lavert, M., Reiner-Benaim, A., Lane, B., Smith, R.S., Savaldi-Goldstein, S., 2021. The root meristem is shaped by brassinosteroid control of cell geometry. Nat. Plants 7, 1475–1484. https://doi.org/10.1038/s41477-021-01014-9.

Geng, Y., Wu, R., Wee, C.W., Xie, F., Wei, X., Chan, P.M.Y., Tham, C., Duan, L., Dinneny, J.R., 2013. A spatio-temporal understanding of growth regulation during the salt stress response in Arabidopsis. Plant Cell 25, 2132–2154. https://doi.org/10.1105/tpc.113.112896.

Gierlinger, N., Keplinger, T., Harrington, M., 2012. Imaging of plant cell walls by confocal Raman microscopy. Nat. Protoc. 7, 1694–1708. https://doi.org/10.1038/nprot.2012.092.

Gieroba, B., Kalisz, G., Krysa, M., Khalavka, M., Przekora, A., 2023. Application of vibrational spectroscopic techniques in the study of the natural polysaccharides and their cross-linking process. Int. J. Mol. Sci. 24, 2630. https://doi.org/10.3390/ijms24032630.

Guo, Q., Liu, L., Barkla, B.J., 2019. Membrane lipid remodeling in response to salinity. Int. J. Mol. Sci. 20, 4264. https://doi.org/10.3390/ijms20174264.

Hauser, F., Horie, T., 2010. A conserved primary salt tolerance mechanism mediated by HKT transporters: a mechanism for sodium exclusion and maintenance of high $K^+$/$Na^+$ ratio in leaves during salinity stress. Plant Cell Environ. 33, 552–565. https://doi.org/10.1111/j.1365-3040.2009.02056.x.

Heath, R.L., Packer, L., 1968. Photoperoxidation in isolated chloroplasts. I. Kinetics and stoichiometry of fatty acid peroxidation. Arch. Biochem. Biophys. 125, 189–198. https://doi.org/10.1016/0003-9861(68)90654-1.

Hu, Y., Xia, S., Su, Y., Wang, H., Luo, W., Su, S., Xiao, L., 2016. Brassinolide increases potato root growth *in vitro* in a dose-dependent way and alleviates salinity stress. BioMed. Res. Int. 2016. https://doi.org/10.1155/2016/8231873. Article ID 8231873.

Ismail, A.M., Horie, T., 2017. Genomics, physiology, and molecular breeding approaches for improving salt tolerance. Annu. Rev. Plant Biol. 68, 405–434. https://doi.org/10.1146/annurev-arplant-042916-04093.

Jin, T., An, J., Xu, H., Chen, J., Pan, L., Zhao, R., Wang, N., Gai, J., Li, Y., 2022. A soybean sodium/hydrogen exchanger GmNHX6 confers plant alkaline salt tolerance by regulating $Na^+$/$K^+$ homeostasis. Front. Plant Sci. 13. https://doi.org/10.3389/fpls.2022.938635.

Kanbar, A., Flubacher, N., Hermuth, J., Kosová, K., Horn, T., Nick, P., 2021. Mining sorghum biodiversity—potential of dual-purpose hybrids for bio-economy. Diversity 13, 192. https://doi.org/10.3390/d13050192 (Basel).

Karlova, R., Boer, D., Hayes, S., Testerink, C., 2021. Root plasticity under abiotic stress. Plant Physiol. 187, 1057–1070. https://doi.org/10.1093/plphys/kiab392.

Khan, T.A., Kappachery, S., Karumannil, S., AlHosani, M., Almansoori, N., Almansoori, H., Yusuf, M., Tran, L.-S.P., Gururani, M.A., 2023. Brassinosteroid signaling pathways: insights into plant responses under abiotic stress. Int. J. Mol. Sci. 24, 17246. https://doi.org/10.3390/ijms24241724.

Khandal, H., Horev, G., van den Herik, B., Soroka, Y., Lahav, T., Avin-Wittenberg, T., ten Tusscher, K., Savaldi-Goldstein, S., 2025. Root growth and branching are enabled by brassinosteroid-regulated growth anisotropy and carbon allocation. Nat. Commun. 16, 3985. https://doi.org/10.1038/s41467-025-59202-6.

Kim, E.J., Russinova, E., 2020. Brassinosteroid signalling. Curr. Biol. 30, R294–R298. https://doi.org/10.1016/j.cub.2020.02.011.

Kraamwinkel, C.T., Beaulieu, A., Dias, T., Howison, R.A., 2021. Planetary limits to soil degradation. Commun. Earth Environ. 2, 249. https://doi.org/10.1038/s43247-021-00323-3.

Lindberg, S., Premkumar, A., 2024. Ion Changes and signalling under salt stress in wheat and other important crops. Plants 13, 46. https://doi.org/10.3390/plants1301004.

Liu, G., Zeng, Y., Li, B., Wang, X., Jiang, L., Guo, Y., 2025. SOS2 phosphorylates FREE1 to regulate multi-vesicular body trafficking and vacuolar dynamics under salt stress. Plant Cell 37. https://doi.org/10.1093/plcell/koaf012.

Ma, L., Li, J., Li, J., Huo, Y., Yang, Y., Jiang, C., Guo, Y., 2026. Plant salt-tolerance mechanisms: classic signaling pathways, emerging frontiers, and future perspectives. Mol. Plant 19, 538–570. https://doi.org/10.1016/j.molp.2025.12.009.

Moreno-Risueno, M.A., Van Norman, J.M., Moreno, A., Zhang, J., Ahnert, S.E., Benfey, P. N., 2010. Oscillating gene expression determines competence for periodic Arabidopsis root branching. Science 329, 1306–1311. https://doi.org/10.1126/science.1191937 (1979).

Mostofa, M.G., Rahman, M.M, Ghosh, T.K., Kabir, A.H., Abdelrahman, M., Rahman Khan, M.A., Mochida, K., Tran, L.S.P., 2022. Potassium in plant physiological adaptation to abiotic stresses. Plant Physiol. Biochem. 186, 279–289. https://doi.org/10.1016/j.plaphy.2022.07.011.

Munns, R., Tester, M., 2008. Mechanisms of salinity tolerance. Annu. Rev. Plant Biol. 59, 651–681. https://doi.org/10.1146/annurev.arplant.59.032607.092911.

Nestrerenko, E.O., Krasnoperova, O.E., Isayenkov, S.V., 2021. Potassium transport systems and their role in stress response, plant growth, and development. Cytol. Genet. 55, 63–79. https://doi.org/10.3103/S0095452721010126.

Noguchi, T., Fujioka, S., Choe, S., Takatsuto, S., Yoshida, S., Yuan, H., Feldmann, K.A., Tax, F.E., 1999. Brassinosteroid-insensitive *dwarf* mutants of Arabidopsis accumulate brassinosteroids. Plant Physiol. 121, 743–752. https://doi.org/10.1104/pp.121.3.743.

Payne, W.Z., Kurouski, D., 2021. Raman spectroscopy enables phenotyping and assessment of nutrition values of plants: a review. Plant Methods 17, 78. https://doi.org/10.1186/s13007-021-00781-y.

Peduzzi, A., Piacentini, D., Brasili, E., Della Rovere, F., Patriarca, A., D'Angeli, S., Altamura, M.M., Falasca, G., 2024. Salt stress alters root meristem definition, vascular differentiation and metabolome in *Sorghum bicolor* (L.) genotypes. Environ. Exp. Bot. 226, 105876. https://doi.org/10.1016/j.envexpbot.2024.105876.

Peduzzi, A., Piacentini, D., D'Angeli, S., Iozia, L.M., Varone, L., Amato, F., Altamura, M. M., Falasca, G., 2025. Brassinosteroid seed priming positively affects leaf anatomy and gas exchanges in a salt-sensitive sorghum genotype exposed to salt stress. Plant Stress 18, 101014. https://doi.org/10.1016/j.stress.2025.101014.

Peethambaran, P.K., Glenz, R., Höninger, S., Shahinul Islam, S.M., Hummel, S., Harter, K., Kolukisaoglu, U., Meynard, D., Guiderdoni, E., Nick, P., Riemann, M., 2018. Salt-inducible expression of *OsJAZ8* improves resilience against salt-stress. BMC Plant Biol. 18, 311. https://doi.org/10.1186/s12870-018-1521-0.

Piacentini, D., Bellini, C., Peduzzi, A., Casentini, B., Tiraboschi, C., Cacciotti, A., Altamura, M.M., Falasca, G., Della Rovere, F., 2024. Arsenite and arsenate stress differently affect auxin distribution in rice roots and brassinosteroids restore it sustaining root system plasticity. Plant Stress 11, 100418. https://doi.org/10.1016/j.stress.2024.100418.

Planas-Riverola, A., Gupta, A., Betegón-Putze, I., Bosch, N., Ibañes, M., Caño-Delgado, A. I., 2019. Brassinosteroid signaling in plant development and adaptation to stress. Development 146, dev151894. https://doi.org/10.1242/dev.151894.

Pound, M.P., French, A.P., Atkinson, J.A., Wells, D.M., Bennett, M.J., Pridmore, T., 2013. RootNav: navigating images of complex root architectures. Plant Physiol. 162, 1802–1814. https://doi.org/10.1104/pp.113.221531.

Riedelsberger, J., Miller, J.K., Valdebenito-Maturana, B., Piñeros, M.A., González, W., Dreyer, I., 2021. Plant HKT channels: an updated view on structure, function and gene regulation. Int. J. Mol. Sci. 22, 1892. https://doi.org/10.3390/ijms22041892.

Saqib, M., Zorb, C., Rengel, Z., Schubert, S., 2005. The expression of the endogenous vacuolar $Na^+/H^+$ antiporters in roots and shoots correlates positively with the salt resistance of wheat (*Triticum aestivum* L.). Plant Sci. 169, 959–965. https://doi.org/10.1016/j.plantsci.2005.07.001.

Schmittgen, T., Livak, K., 2008. Analyzing real-time PCR data by the comparative CT method. Nat. Protoc. 3, 1101–1108. https://doi.org/10.1038/nprot.2008.73.

Shahbaz, M., Ashraf, M., 2007. Influence of exogenous application of brassinosteroid on growth and mineral nutrients of wheat (*Triticum aestivum* L.) under saline conditions. Pak. J. Bot. 39, 513.

Sharma, I., Ching, E., Saini, S., Bhardwaj, R., Kumar Pati, P., 2013. Exogenous application of brassinosteroid offers tolerance to salinity by altering stress responses in rice variety Pusa Basmati-1. Plant Physiol. Biochem. 69, 17–26. https://doi.org/10.1016/j.plaphy.2013.04.013.

Shi, H., Zhu, J.K., 2002. Regulation of expression of the vacuolar $Na^+/H^+$ antiporter gene *AtNHX1* by salt stress and abscisic acid. Plant Mol. Biol. 50, 543–550. https://doi.org/10.1023/a:1019859319617.

Singh, V., van Oosterom, E.J., Jordan, D.R., Messina, C.D, Cooper, M., Hammer, G.L., 2010. Morphological and architectural development of root systems in sorghum and maize. Plant Soil 333, 287–299. https://doi.org/10.1007/s11104-010-0343-0.

Smilde, A.K., Jansen, J.J., Hoefsloot, H.C., Lamers, R.J.A., Van Der Greef, J., Timmerman, M.E., 2005. ANOVA-simultaneous component analysis (ASCA): a new tool for analyzing designed metabolomics data. Bioinformatics 21, 3043–3048. https://doi.org/10.1093/bioinformatics/bti476.

Song, Y.L., Dong, Y.J., Tian, X.Y., Kong, J., Bai, X.Y., Xu, L.L., He, Z.L., 2016. Role of foliar application of 24-epibrassinolide in response of peanut seedlings to iron deficiency. Biol. Plant. 60, 329–342. https://doi.org/10.1007/s10535-016-0596-4.

Stevens, J.P., 2007. Intermediate Statistics: A Modern Approach, 3rd ed. Lawrence Erlbaum Associates Publishers.

Sunarpi, Horie T., Motoda, J., Kubo, M., Yang, H., Yoda, K., Horie, R., Chan, H.Y., Leung, H.Y., Hattori, K., Konomi, M., Osumi, M., Yamagami, M., Shroeder, J.I., Uozumi, N., 2005. Enhanced salt tolerance mediated by AtHKT1 transporter-induced $Na^+$ unloading from xylem vessels to xylem parenchyma cells. Plant J. 44, 928–938. https://doi.org/10.1111/j.1365-313X.2005.02595.x.

Tanveer, M., Shahzad, B., Sharma, A., Biju, S., Bhardwaj, R., 2018. 24-Epibrassinolide; an active brassinolide and its role in salt stress tolerance in plants: a review. Plant Physiol. Biochem. 130, 69–79. https://doi.org/10.1016/j.plaphy.2018.06.035.

Tariq, F., Zhao, L., Hussain, S., Riaz, M.W., Wu, C., Zhang, J., Gangurde, S.S., 2026. Plasticity and adaptive architecture of roots for enhanced salinity tolerance in crops. Biotechnol. Adv. 87, 108773. https://doi.org/10.1016/j.biotechadv.2025.108773.

van den Berg, T., Yalamanchili, K., de Gernier, H., Santos Teixeira, J., Beeckman, T., Scheres, B., Willemsen, V., ten Tusscher, K., 2021. A reflux-and-growth mechanism explains oscillatory patterning of lateral root branching sites. Dev. Cell 56, 2176–2191. https://doi.org/10.1016/j.devcel.2021.07.005 e10.

van Zelm, E., Zhang, Y., Testerink, C., 2020. Salt tolerance mechanisms of plants. Annu. Rev. Plant Biol. 71, 403–433. https://doi.org/10.1146/annurev-arplant-050718-100005.

Vardhini, B.V., Anjum, N.A., 2015. Brassinosteroids make plant life easier under abiotic stresses mainly by modulating major components of antioxidant defense system. Front. Environ. Sci. 2, 67. https://doi.org/10.3389/fenvs.2014.00067. Article.

Veerman, C., Pinto Correia, T., Bastioli, C., Biro, B., Bouma, J., Cienciala, E., Emmett, B., Frison, E.A., Grand, A., Lachezar, Hristov, Kriaučiūnienė, Zita, Pogrzeba, M., Soussana, J.F., Vela, C., Wittkowski, R., 2020. Caring for soil is caring for life – Ensure 75% of soils are healthy by 2030 for healthy food, people, nature and climate. Eur. Comm. Rep. 2020. https://doi.org/10.2777/4833.

Vis, D.J., Westerhuis, J.A., Smilde, A.K., van der Greef, J., 2007. Statistical validation of megavariate effects in ASCA. BMC Bioinform. 8, 322. https://doi.org/10.1186/1471-2105-8-322.

Waheed, A., Zhuo, L., Wang, M., Hailiang, X., Tong, Z., Wang, C., Aili, A., 2024. Integrative mechanisms of plant salt tolerance: biological pathways, phytohormonal regulation, and technological innovations. Plant Stress 14, 100652. https://doi.org/10.1016/j.stress.2024.100652.

Wang, S., Liu, D., Jin, T., Du, J., Tian, A., Huang, Q., Khan, M., Nie, S., Zhang, S., Deng, R., Zhang, M., Wang, X., 2023a. Manipulation of brassinosteroid signaling via overexpression of its major receptor SlBRI1 regulates salt tolerance in tomato. Sci. Hortic. 322, 112457. https://doi.org/10.1016/j.scienta.2023.112457.

Wang, X., Chai, J., Liu, W., Zhu, X., Liu, H., Wei, X., 2023b. Promotion of $Ca^{2+}$ accumulation in roots by exogenous brassinosteroids as a key mechanism for their enhancement of plant salt tolerance: a meta-analysis and systematic review. Int. J. Mol. Sci. 24, 16123. https://doi.org/10.3390/ijms242216123.

Wang, Z.Y., Nakano, T., Gendron, J., He, J., Chen, M., Vafeados, D., Yang, Y., Fujioka, S., Yoshida, S., Asami, T., Chory, J., 2002. Nuclear-localized BZR1 mediates brassinosteroid-induced growth and feedback suppression of brassinosteroid biosynthesis. Dev. Cell 2, 505–513. https://doi.org/10.1016/s1534-5807(02)00153-3.

Wu, H., Shabala, L., Liu, X., Azzarello, E., Zhou, M., Pandolfi, C., Chen, Z.H, Bose, J., Mancuso, S., Shabala, S., 2015. Linking salinity stress tolerance with tissue-specific Na+ sequestration in wheat roots. Front. Plant Sci. 6, 71. https://doi.org/10.3389/fpls.2015.00071.

Yamagami, A., Chieko, S., Sakuta, M., Shinozaki, K., Osada, H., Nakano, A., Asami, T., Nakano, T., 2018. Brassinosteroids regulate vacuolar morphology in root meristem cells of Arabidopsis thaliana. Plant Signal. Behav. 13, e1417722. https://doi.org/10.1080/15592324.2017.1417722.

Zhang, J., Hou, L., Guo, X., Zhi, M., Sun, S., Sun, Y., Wang, X., Zhang, D., Wang, J., Kang, Z., Ni, Z., Ji, W., Li, T., Xu, S., 2026. TaGSK3 controls wheat lateral root developmental plasticity under salt stress. Crop J. 14, 362–373. https://doi.org/10.1016/j.cj.2025.11.012.

Zhang, J., Cai, J., Xu, D., Wu, B., Chang, H., Zhang, B., Wei, Z., 2024. Soil salinization poses greater effects than soil moisture on field crop growth and yield in arid farming areas with intense irrigation. J. Clean. Prod. 451, 142007. https://doi.org/10.1016/j.jclepro.2024.142007.

Zhang, L., Ma, H., Chen, T., Pen, J., Yu, S., Zhaoe, X., 2014. Morphological and physiological responses of cotton (*Gossypium hirsutum* l.) plants to salinity. PLoS One 9, e112807. https://doi.org/10.1371/journal.pone.0112807.

Zhang, S., Hu, J., Zhang, Y., Xie, X.J., Knapp, A., 2007. Seed priming with brassinolide improves lucerne (*Medicago sativa* L.) seed germination and seedling growth in relation to physiological changes under salinity stress. Aust. J. Agric. Res. 58, 811–815. https://doi.org/10.1071/AR06253.

Zeise, I., Heiner, Z., Holz, S., Joester, M., Büttner, C., Kneipp, J., 2018. Raman imaging of plant cell walls in sections of *Cucumis sativus*. Plants 7, 7. https://doi.org/10.3390/plants7010007.